İSTANBUL TECHNICAL UNIVERSITY ★ INSTITUTE OF SCIENCE AND TECHNOLOGY

A THEORETICAL STUDY ON Ru CATALYZED AZIDE ALKYNE CYCLOADDITION

M.Sc. Thesis by
Esra BOZ

Department : Chemistry

Programme : Chemistry

JUNE 2011

İSTANBUL TECHNICAL UNIVERSITY ★ INSTITUTE OF SCIENCE AND TECHNOLOGY

A THEORETICAL STUDY ON Ru CATALYZED AZIDE ALKYNE CYCLOADDITION

M.Sc. Thesis by
Esra BOZ
(509091040)

Date of submission : **06 May 2011**
Date of defence examination: **07 June 2011**

Supervisor (Chairman) : **Assoc. Prof. Dr. Nurcan TÜZÜN (ITU)**
Members of the Examining Committee: **Prof. Dr. Emine Naciye TALINLI (ITU)**
Prof. Dr. Safiye ERDEM (MU)

JUNE 2011

İSTANBUL TEKNİK ÜNİVERSİTESİ ★ FEN BİLİMLERİ ENSTİTÜSÜ

Ru KATALİZÖRLÜ AZİT ALKİN SİKLOKATILMA TEPKİMELERİ ÜZERİNE HESAPSAL BİR ÇALIŞMA

YÜKSEK LİSANS TEZİ

Esra BOZ
(509091040)

Tezin Enstitüye Verildiği Tarih: 06 Mayıs 2011
Tezin Savunulduğu Tarih: 07 Haziran 2011

Tez Danışmanı : Doç. Dr. Nurcan TÜZÜN (İTÜ)
Diğer Jüri Üyeleri: Prof. Dr. Emine Naciye TALINLI (İTÜ)
Prof. Dr. Safiye ERDEM (MÜ)

HAZİRAN 2011

FOREWORD

I wish to express my appreciation to Assoc. Prof. Dr. Nurcan TÜZÜN, for supporting and giving advice to me from the beginning of this thesis.

My special thanks to my family, who give their support and love; and for their guidance in my whole life.

June 2011

Esra BOZ
Chemist

TABLE OF CONTENTS

Page

ABBREVIATIONS

B3LYP	**:** Becke Style Three Parameter Functional in Combination with the Lee-Yang Parr Correlation Functional
DFT	**:** Density Functional Theory
E	**:** Energy
G03	**:** Gaussian 03
H	**:** Hamiltonian Operator
HF	**:** Hartree-Fock
IRC	**:** Intrinsic Reaction Coordinate
LDA	**:** Local Density Approximation
NBO	**:** Natural Bond Orbital

LIST OF TABLES

Page

LIST OF FIGURES

Page

A THEORETICAL STUDY ON Ru CATALYZED AZIDE ALKYNE CYCLOADDITION REACTION

SUMMARY

1,2,3-triazoles are a member of azole family, which have been widely used in especially biomedical applications. One of the synthetic methods to assemble 1,2,3-triazoles is the Huisgen 1,3-dipolar cycloaddition of azides and alkynes. This reaction has a high activation barrier and it is very slow even at high temperatures. An alternative and a very recent method of obtaining 1,5-disubstituted triazoles is via ruthenium catalyzed reaction of alkynes with azides. In this study, a ruthenium catalyzed azide-alkyne cycloaddition reaction has been modeled by quantum mechanical methods. Firstly, a model mechanism has been devised and a pathway for the reaction has been found. Then, the reaction of azide-alkyne with different substituents based on experimental work has been modeled by following model mechanism. Additionally, the effect of the catalyst has been investigated by adding a different ligand on the Ru metal. For this purpose, DFT calculations have been performed with the B3LYP functional with the 6-31G* basis set, utilizing Gaussian 03 program package. To account on the effect of substrate, two other systems, where the alkyne is substituted with alcohol and ketone functional groups have also been modeled and compared with the experimental results. The calculations in this study have reproduced the experimental regioselectivity and allowed us to account on the effects employed in this study. Both thermodynamic and kinetic parameters appeared to be important in these reactions. The thermodynamic stability of the complexes and the relative ease of the complex to undergo reaction determines the product distribution.

Ru KATALİZÖRLÜ AZİT ALKİN SİKLOKATILMA TEPKİMELERİ ÜZERİNE HESAPSAL BİR ÇALIŞMA

ÖZET

1,2,3-triazoller azol ailesinin bir üyesidir ve özellikle biyomedikal alanında uygulamaları mevcuttur. Triazollerin elde yöntemlerinden biri Husigen'in azit ve alkinlerin 1,3-dipolar siklokatılma tepkimesidir. Bu tepkime hem yüksek aktivasyon bariyerine sahiptir, hem de yüksek sıcaklıklarda bile yavaş ilerlemektedir. 1,5-triazollerin rutenyum katalizörlüğünde azit ve alkinlerin tepkimesinden elde edilmesi alternatif ve yeni bir yoldur. Bu çalışmada rutenyum katalizörlü bir azit-alkin siklokatılma tepkimesi kuantum mekanik metodlarla modellenmiştir. İlk olarak model bir tepkime önerilmiş ve tepkime mekanizması bulunmuştur. Daha sonra deneysel olarak çalışılmış farklı sübstitüentli azit-alkin molekülleri içeren gerçek bir sistem model tepkime kullanılarak modellenmiştir. Bunun yanında, katalizörün tepkimedeki etkisinin anlaşılması için farklı bir ligand içeren Ru metalli tepkime incelenmiştir. Bu amaçla B3LYP fonksiyoneli ile YFT teorisi kullanılarak 6-31G* bazında Gaussian 03 programı kullanılarak hesaplamalar gerçekleştirilmiştir. Substratın etkisini açıklamak için alkol ve keton grupları içeren iki farklı sistem daha modellenmiş ve sonuçlar deneysel verilerle karşılaştırılmıştır. Hesaplamalarda, deneysel olarak görülen regioseçicilik desteklenmektedir. Bu reaksiyonlarda hem kinetik hem de termodinamik parametrelerin önemli olduğu görülmektedir. Ürün dağılımını, hem komplekslerin termodinamik kararlılıkları, hem de komplekslerin reaksiyon verme kolaylıkları etkilemektedir.

1. INTRODUCTION

1,2,3-triazoles, the subject of this thesis, is a member of azole family, which have been widely used in especially biomedical applications, yet not benefitted widely. The 1,2,3-triazole heterocycle has different advantageous properties. Their high chemical stability provide them to being inert to severe hydrolytic, oxidizing and reducing conditions, even at high temperatures. It has aromatic character, a strong dipole moment (4.8-5.6 Debye), and hydrogen bond accepting ability. Therefore, it can interact productively with biological molecules, materials, organic and inorganic molecules in various ways [1-6]. Triazoles show high biological activity, thus they are utilized in the treatment of tumors [7-8], HIV [9], allergy [10], fungal infection [11-12] and microbial [13-17] diseases. Recently, it has been found that triazoles are effective to reduce activity of liver catalase and inhibit the production of liver cancer [18]. Several triazole derivatives prohibit the propagation of the infected cells and facilitate the control of breast cancer [19,20]. Similarly, at the prostate and pancreatic cancer cases they are efficient to heal infected cells and prevent permeation of illness [21].

One of the synthetic methods to assemble 1,2,3-triazoles is the Huisgen 1,3-dipolar cycloaddition of azides and alkynes (AAC) [22-23]. This reaction has a high activation barrier, allthough it is exothermic, so the reaction rate is very low even at high temperatures. This slow cycloaddition is directly related to the kinetic stability of alkynes and azides [22-28]. Since the differences in HOMO-LUMO energy levels for both azides and alkynes are of similar magnitude, both dipole-HOMO- and dipole-LUMO-controlled pathways operate in these cycloaddition [29]. As a result, when an unsymmetrical alkyne is used, a regioisomeric 1,2,3-triazole mixture of 1:1 ratio 1,4- and 1,5-disubstituted-1,2,3-triazoles is formed [30,31].

In 2001, the copper-catalyzed 1,3-dipolar *a*zide-*a*lkyne *c*ycloaddition (CuAAC) process has emerged as the premier example of click chemistry by Sharpless to describe a set of 'near-perfect' bond-forming reactions, useful for rapid assembly of molecules with desired function [32].

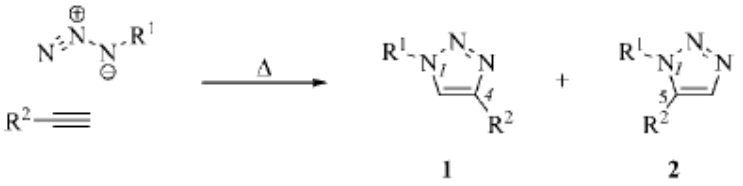

Figure 1.1 : Products of thermal 1,3 – cycloaddition

The main advantages of this reaction are reported independently by the Sharpless [33] and Meldal [34] groups. Click transformations give rise to products in very high yields with little or no byproducts and are easily performed. Cu(I) catalysis increases the reaction rate up to 10^7 times [35] compared to the uncatalyzed process and eliminates the need for elevated temperatures. The process is not significanly affected by the steric and electronic properties of the groups attached to the alkyne and azide centers and proceeds well in many protic and aprotic solvents including water [36]. Variously substituted terminal alkynes generally react well with several types of azides including primary, secondary, tertiary, electron-defficient and electron-rich, aliphatic, aromatic and heteroaromatic azides. The activation barrier for the catalyzed reaction is lower than the uncatalyzed reaction because of the stepwise cycloddition observed in the Cu(I) catalysis. This stepwise process increases the reaction rate extremely [37]. Additionally, internal alkynes are not active in CuAAC reactions, because stepwise catalytic cycle is thought to begin with deprotonation of the alkyne to form Cu^I acetylide.

The success of the copper catalyst has invoked the scientists to work on different metal analogues. Several metals which are effective in alkyne transformation reactions have been tested and have not given satisfactory results in azide alkyne cycloaddition. In addition to first-row transition metals, Ag(I), Pd(0/II), Pt(II), Au(I/III) and Hg(II) have also been analyzed, however reasonable yield, rate increase or selectivity have not been observed [36]. Only CuAAC reaction succesfully provides 1,4-disubstituted 1,2,3-triazoles, yet a method to produce the 1,5-disubstituted regioisomer is still needed.

The catalytic effect of ruthenium complexes on alkynes are known, so several ruthenium complexes have been searched for a catalyst of azide–alkyne cycloaddition. In 2005, ruthenium catalysis was found as a complementary reaction to CuAAC which has a different regioselectivity. By using Ru catalyst, 1,5disubstituted triazoles are synthesized and as an improvement, this reaction is

available with internal alkynes. However, there are some uncertain points about the mechanism of Ru cycloaddition.

It has been shown by the experiments that the catalytic activity and regioselectivity of the Ru complexes differ with the ligands around the central metal atom. For example, an acetate complex ligand like $Ru(OAc)_2(PPh_3)_2$ gives completely 1,4-disubstituted triazole product. The yield of this reaction is 46% and any 1,5-disubstituted triazole product has not been detected. $RuCl_2(PPh_3)_3$ and RuHCl(CO) $(PPh_3)_3$ complexes have also given 1,4-disubstituted triazole with less than a 5% yield. Similarly, they produce a trace amount of 1,5-disubstituted triazoles or none.

When cyclopentadiene (Cp) ligand is used with Ru, a mixture of 1,4 and 1,5-disubstituted triazoles can be obtained if the reaction takes place [38]. Switching Cp component to Cp* (the pentamethyl analogue of Cp) resulted 100% conversion to 1,5-disubstituted triazole.

Adding several ligands to [Cp*Ru] complex gives similar results to obtain 1,5-disubstituted triazoles (Figure 1.1) [29]. The table shows that the catalysts with Cp* ligand show excellent yields producing 1,5-disubstituted triazole.

Table 1.1: Performance of Ruthenium(II) Catalysts in Cycloaddition of Benzyl Azide and Phenyl Acetylene in THF.

Ru catalyst	**1,5**	**1,4**
$CpRuCl(PPh_3)_2$	13%	1%
$Cp^*RuCl(PPh_3)_2$	100%	-
Cp*RuCl(COD)	93%	-
Cp*RuCl(NBD)	100%	-
$[Cp^*RuCl]_4$	100%	-

In most of the cases, the catalytic reactions are used as black boxes. The efficiency and the wide usage of the click reactions have ended up with many work in the literature. However, the details of the mechanism is unclear. In the case of ruthenium, experimentalists have proposed a tentative reaction mechanism. The aim of this study is to elucidate the reaction mechanism of Ru catalyzed azide-alkyne reaction and to explain the effect of the catalyst on the mechanism. With this aim, a set of Ru-catalyzed azide-alkyne reaction has been studied by quantum mechanical methods. First, a model reaction has been devised in order to test the effect of the methyl groups on the cyclopentadienyl ligand. $Cp^*RuCl(PPh_3)_2$ has given 1,5-disubstituted triazole compound whereas the absence of methyl groups on

cyclopentadienyl ring has resulted with a mixture of 1,4- and 1,5-disubstituted triazole products if the reaction takes place [29,38].

Later, the model has been applied to a real system that has been experimentally studied. The experimental work involves the reaction of benzyl azide and phenylacetylene in the presence of $Cp^*RuCl(PPh_3)_2$ catalyst (shown in Figure 1.2) [38].

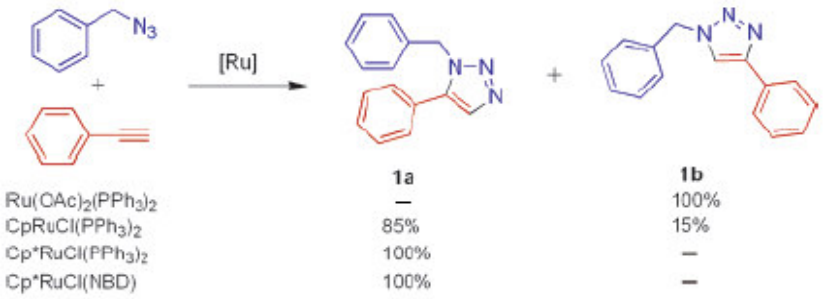

Figure 1.2 : Ru-Catalyzed Cycloaddition of Benzyl Azide and Phenylacetylene

In the last part of the work, the study is extended to a set of experiments where different functional groups enabled products of different regioselectivities (Figure 1.3 entries 2- 3).

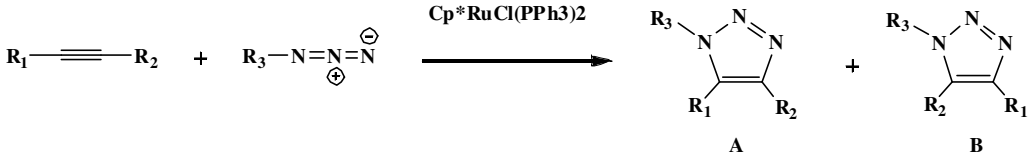

entry	R1	R2	R3	A:B	
model	H	CH_3	CH_3	No exp. data	model C
1	H	Ph	CH_2Ph	0:100	RC1
2	Ph	CH_2OH	CH_2Ph	0:100	RC2
3	Ph	COMe	CH_2Ph	100:0	RC3
4	Ph	CH_3	CH_2Ph	38:62	

Figure 1.3 : Modelled reactions and their products

These efforts will enable to shed light on the reaction mechanism in detail. In this work, this proposal and the possible competing pathways have been analyzed and

discussed in detail. This effort is important in the sense that finding the reaction mechanism will enable one to play with the effects and lead to obtain tailor-made products.

2. THEORY

The electronic structure methods use the laws of quantum mechanics. The energy and other related properties of a system may be obtained by solving the Schrödinger equation for this system:

$$\mathbf{H}\Psi = E\Psi \qquad \textbf{(2.1)}$$

where, Ψ is a wavefunction describing the x, y and z spatial coordinates of the particles in the system, E is the energy of the system at that state and **H** is the Hamiltonian operator to derive the kinetic and potential energy of a system. Calculating the exact solution of Schrödinger equation is almost impossible and computationally impractical. Therefore, in electronic structure methods, some approximations are used. The mostly encountered three major classes of electronic structure methods are:

- Semi-empirical methods, they use parameters derived from experimental data. Different semi-empirical methods are characterized by their different parameters.
- Ab initio methods, no experimental parameters are used.
- Density functional methods, the total energy of the system only depends on the electron density.

2.1 Semi-empirical Theory and Ab-initio Methods

In ab initio method, the Hamiltonian and the wavefunction (Ψ) have been defined, the effective electronic energy can be found by use of the variational method. In the variational method, the best wavefunction is found by minimizing the effective electronic energy with respect to parameters in the wavefunctions.

The accuracy of this method depends on the chosen wavefunction. However, with increasing molecule size and complexity of wavefunction, ab calculations become more expensive computationally [39].

The difficulty of performing ab-initio calculations on large molecules led to develop semi-empirical methods. In this method, rather than solving all the integrals of the

Schrödinger equation, parameters originating from experimental data are used. Semi-empirical models can be used to yield continuous energy surfaces. They are neither variational nor size consistent. More importantly, semi-empirical methods are inherently dependent on the choice of parameters. The parameterization is tested against a limited set of molecules to ensure its accuracy. This dependence on parameters can be minimized by using a large and varied training set of molecules to establish parameters. This process is a continuing one. Parameters are introduced in order to reproduce experimental equilibrium geometries, heats of formation, electric dipole moments and ionization potentials.

2.2 Density Functional Theory

Density Functional Theory (DFT) is a theory in which ground state energy is expressed in terms of electron density [40-43]. This method was proposed by P. Hohenberg and W. Kohn in 1964 but it contained only virtual functionals. In 1965, Kohn and Sham brought formal functionals based on total electron density. Contrary to Hartree-Fock method [44-46], DFT has smaller computational cost with high accuracy. Although both methods account for the instantaneous interactions of pairs of electrons with opposite spin, DFT methods include the effects of electron correlation (electrons in a molecular system react to one another's motion and attempt to keep out of another's way) while Hartree-Fock calculations see this effect in an average sense (each electron sees and reacts to an averaged electron density).

Density functional methods partition the electronic energy into several terms and compute them separately.

$$E = E_T + E_V + E_J + E_{XC} \qquad \textbf{(2.2)}$$

E_T is the kinetic energy term, E_V is the potential energy of the nuclear-electron attraction and nuclear-nuclear repulsion term, E_J is the electron-electron repulsion term (also called Coulomb energy), E_{XC} is the exchange-correlation term that includes the remaining part of the electron-electron interactions and it is not known how to calculate exactly.

All the terms except the nuclear-nuclear repulsion, are functions of electron density, $\rho(r)$. E_{XC} can be categorized into exchange and correlation functionals. E_{XC} accounts for the exchange energy arising from the antisymmetry of the quantum mechanical wavefunction and the dynamic correlation in the motions of the individual electrons.

The variational principle determines the ground state energy and electron density in terms of the electron density. Further, the ground state electron density $\rho(r)$ determines the external potential, $v(r)$ and variationally determines the ground state properties of the system of interest.

The electronic energy can be expressed as a functional of the electron density:

$$E[\rho] = \int v(r)\rho(r)dr + T[\rho] + V_{ee}[\rho] \qquad \textbf{(2.3)}$$

where $T[\rho]$ is the kinetic energy of interacting electrons and $V_{ee}[\rho]$ is the interelectronic interactions.

The electronic energy may be written in the form of Kohn-Sham approach.

$$E[\rho] = \int v(r)\rho(r)dr + T_s[\rho] + J[\rho] + E_{xc}[\rho] \qquad \textbf{(2.4)}$$

This is based upon an orbital density description that removes the necessity of knowing the exact form of $T[\rho]$. Kohn-Sham proposed focusing on the kinetic energy of non-interacting system of electrons $T_s[\rho]$, as a functional of a set of single particle orbitals that give exact density.

$$T_s[\rho] = \sum_{i=1}^{N} \langle \Psi_i | -\frac{1}{2}\nabla^2 | \Psi_i \rangle \qquad \textbf{(2.5)}$$

$J[\rho]$ represents the electron-electron repulsion (Coulomb energy), and $E_{xc}[\rho]$ is the exchange-correlation energy functional with its functional derivative called the exchange-correlation potential, $v_{xc}(r)$.

$$E_{xc}[\rho] = T[\rho] - T_s[\rho] + V_{ee}[\rho] - J[\rho] \qquad \textbf{(2.6)}$$

$$v_{xc}(r) = \frac{\partial E_{xc}[\rho]}{\partial \rho(r)} \qquad \textbf{(2.7)}$$

$E_{xc}[\rho]$ is divided into two parts, namely an exchange functional, $E_x[\rho]$ and a correlation functional, $E_c[\rho]$.

$$E_{xc}[\rho] = E_x[\rho] + E_c[\rho] \tag{2.8}$$

$E_x[\rho]$ and $E_c[\rho]$ functionals can be both local and gradient-corrected functionals. Local or gradient-corrected functionals are called traditional functionals. Local functionals depend only on electron density ρ, while gradient-corrected fuctionals depend on both ρ and its gradient, $\Delta\rho$.

A system of non-interacting electrons moving in an external effective potential $v_{eff}(r)$ is shown as;

$$v_{eff}(r) = v(r) + \frac{\partial J[\rho]}{\partial \rho(r)} + \frac{\partial E_{xc}[\rho]}{\partial \rho(r)} = v(r) + \int \frac{\rho(r')}{|r - r'|} dr' + v_{xc}(r) \tag{2.9}$$

Now, an equation very similar to the Schrödinger Equation exists.

$$\left[-\frac{1}{2}\nabla^2 + v_{eff}(r) \right] \Psi_i = \varepsilon_i \Psi_i \tag{2.10}$$

(2.4), (2.5), (2.6), (2.7), (2.8), (2.9) are Kohn-Sham Equations.

In order to evaluate the exchange-correlation functional some approximations are made. The first one is the local density approximation (LDA). It is based upon a model of uniform electron gas. In the uniform electron gas model, a large number of electrons uniformly spread out in a cube where there is a uniform distribution of the positive charge to make the system neutral. It assumes that the charge density varies slowly throughout the molecule so that a localized region of the molecule behaves like a uniform electron gas The energy expression is:

$$E[\rho] = T_s[\rho] + \int \rho(r) v(r) dr + J[\rho] + E_{xc}[\rho] + E_b \tag{2.11}$$

where E_b is the electrostatic energy of the positive background. Since the positive charge density is the negative to the electron density, the equation reduces to:

$$E[\rho] = T_s[\rho] + E_{xc}[\rho] = T_s[\rho] + E_x[\rho] + E_c[\rho] \tag{2.12}$$

The exchange functional is given by:

$$E_x[\rho] = -C_x \int \rho(r)^{4/3} dr \qquad \textbf{(2.13)}$$

C_x=0.7386, this form was developed to reproduce the exchange energy of a uniform electron gas.

DFT methods are defined by pairing an exchange functional with a correlation functional and can be named as traditional or hybrid functionals. Hybrid functionals include exact term in the exchange functional, whereas traditional functionals do not. BLYP (Becke's gradient-corrected exchange functional with Lee-Yang-Parr's gradient-corrected correlation functional) method is a traditional functional whereas, B3LYP (Becke style three parameter functional in combination with the Lee-Yang-Parr correlation functional) method [47], the linear combination of LDA, B88, exact and LYP functionals, is a hybrid functional:

$$E_{xc} = E_{xc}^{LDA} + a_0(E_x^{exact} - E_x^{LDA}) + a_x \Delta E_x^{B88} + a_c \Delta E_c^{non-local} \qquad \textbf{(2.14)}$$

where ΔE_x^{B88} is the Becke's gradient correction, i.e. the second term at the right hand side of the equation (2.12) and the correction to the correlation ($\Delta E_c^{non-local}$) is provided by the Lee-Yang-Parr functional. But, LYP includes both local and non-local terms, then the correlation functional used is actually: $a_c E_c^{LYP} + (1 - a_c) E_c^{VWN}$ where E_c^{VWN} is the Vosko-Wilk-Nusair correlation energy. The parameters are specified by Becke by fitting the atomization energies, ionization potentials, proton affinities and first row atomic energies in the molecule set, a_0=0.20, a_x=0.72 and a_c=0.81. Hybrid functionals have proven to be superior to the traditional functionals.

2.2.1 Basis sets

A basis set is a serie of basis functions which is used to expressed molecular orbitals. The molecular orbitals are emphasized as a linear combination of basis funtions which are pre-defined one-electron atomic functions. The basis functions are categorized into

two classes, Slater Type Orbitals (STO) and Gaussian Type Orbitals (GTO). Slater Type Orbitals have the functional form

$$\Theta_{abc}(x,y,z) = N x^a y^b z^c e^{-\zeta r} \qquad \textbf{(2.15)}$$

N is the normalization constant, a, b and c are angular momentum (L= a+b+c). Gaussian type orbitals can be written as

$$\Theta_{abc}(x,y,z) = Nx^a y^b z^c e^{-\zeta r^2} \quad \textbf{(2.16)}$$

GTOs are preferable over STOs because of the computational efficiency although STOs are more accurate. Among the types of the basis sets (minimal basis sets, split valence basis sets, polarized basis sets, high angular momentum basis sets) the most popular one is the split valence basis set which is developed by Pople and his group termed as 3-21G, 4-31G, 6-31G. Split valence basis sets allow orbitals to change size but not the shape. Polarized basis sets remove this limitation by adding orbitals with angular momentum beyond the ground state configuration for each atom. In this study 6-31G*, also known as 6-31G(d) polarization basis set is used where d functions are added to heavy atoms [48].

2.2.2 Intrinsic reaction coordinate

Intrinsic Reaction Coordinate (IRC) [49-50] is a minimum energy reaction path on a potential energy surface in mass-weighted coordinates, connecting reactants to products via the transition state [51]. When a transition state is optimized with an imaginary frequency, it must be confirmed that it is the correct transition state by making IRC calculations. The IRC path is defined by the differential equation

$$\frac{d\mathbf{x}}{ds} = - \frac{\mathbf{g}}{|\mathbf{g}|} = \mathbf{v} \quad \textbf{(2.17)}$$

Where x is the mass-weighted coordinates, s is the path length and v is the negative normalized gradient [48].

2.2.3 Natural bond orbital

Natural Bond Orbital (NBO) [52-59] analysis is the diagonalization of first-order density matrix which is used to define character of bonds and orbitals. Let A, B and C are the atoms of a molecule. The density matrix can be written in terms of blocks of basis functions belonging to a specific centre as,

$$D = \begin{pmatrix} D^{AA} & D^{AB} & D^{AC} & \ldots \\ D^{AB} & D^{BB} & D^{BC} & \ldots \\ D^{AC} & D^{BC} & D^{CC} & \ldots \\ \ldots & \ldots & \ldots & \ldots \end{pmatrix} \quad \textbf{(2.18)}$$

NBO for A can be defined as diagonalization of the D^{AA} block. The same process is valid for B by D^{BB} block and C by D^{CC} block. NBOs are not orthogonal and orbital occupation numbers are not the total number of electrons [48].

3. METHODOLOGY

In this study, reaction mechanisms have been modeled and discussed in terms of relative energies obtained from quantum mechanical calculations. Intermediates and transition state structures have been optimized by the B3LYP functional with the 6-31G* basis set [60-62]. For Ru, LANL2DZ effective core potential has been used. In the literature it is stated that this methodology gives succesfull results for Ru metal and these atoms [29]. For DFT calculations Gaussian 03 package has been utilized [63].

The stationary points were analyzed by vibrational frequency calculations. All transition states were verified to be saddle points by one imaginary frequency belonging to the reaction coordinate.

IRC calculations have been performed on transition states to obtain minima on both sides [64-65]. The energies of the starting complexes are discussed in terms of electronic energies. The energies discussed in the reaction coordinates are Gibbs free energies calculated at 298 K, unless otherwise stated.

NBO analysis has been carried out on some structures in order to investigate the stabilizing donor-acceptor interactions and the nature of the Ru-C bonds in some selected structures [66-70].

4. RESULTS AND DISCUSSION

To elucidate the RuAAC reaction mechanism and the effect of ligands and the substrate on the regioselectivity, the reaction shown in Figure 4.1 has been modeled by the DFT calculations. The study will be divided into two parts:

1. The effect of substrate

2. The effect of the ligand on catalyst

The effect of [Cp*RuCl(PPh_3)$_2$] catalyst on the distribution of triazole product will be investigated. At the first part, the role of the Cp and Cp* rings on Ru metal will be discussed. According to the experimental study reported by Boren et al., [Cp*RuCl] complexes were found to be active and selective catalysts for the reaction between benzyl azide and phenyl acetylene. Switching the Cp* ring to Cp, the product ratio of 100:0 will be decreased to 85:15.

At the second part, the effect of substrate with [Cp*RuCl(PPh_3)$_2$] catalyst on the distribution of triazole product will be investigated (Figure 1.3, entries model and 1). The trisubstituted triazoles reported by Majireck et al. gives different ratios of 1,4,5 triazoles with the same catalyst [71]. As a further work, steric and electronic effects of the reactants which enable regioselective synthesis will be investigated (Figure 1.3, entries 2 and 3).

A mechanism has been proposed by the experimentalists in the literature (Figure 4.1) [29].

At Step A, spectator ligands are displaced and azide-alkyne groups are coordinated to the Ru catalyst. After this step terminal nitrogen atom on the azide group attacks to the alkyne and a ruthenacycle intermediate is formed. At step C, alkyne group is seperated from the Ru metal and bonded to the nitrogen atom to form a triazole ring. At the last step, triazole is departed from the catalyst and the catalyst is regenerated.

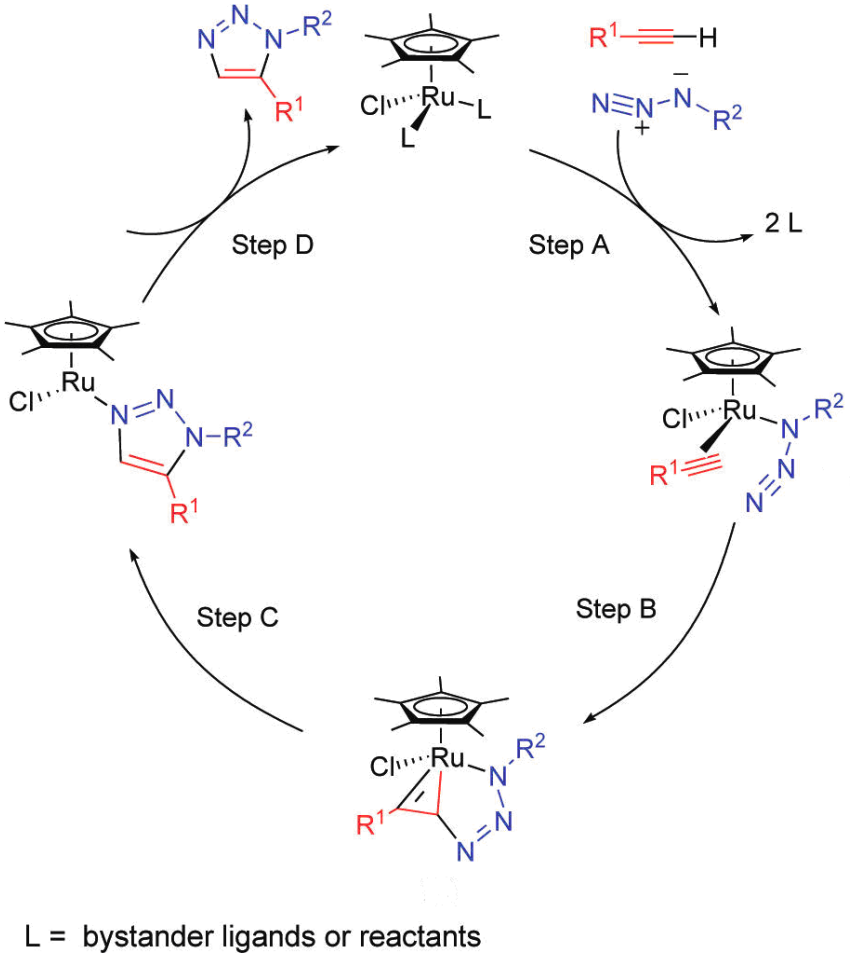

Figure 4.1 : Catalytic cycle of the RuAAC reaction [29].

4.1 Model Reaction

In the first part of this study, a model reaction has been studied in order to eliminate the steric effects and to solely concentrate on the electronic properties of the reaction mechanism. For this purpose, the uncatalyzed and ruthenium catalyzed reactions of methyl-azide and propyne (Entry model, Figure 4.1) have been modeled by the DFT calculations.

Uncatalyzed :

The uncatalyzed reactions of 1,3-dipolar cycloadditions reveal a mixture of regioisomeric products since the HOMO and LUMO of diene and dienophile are close in energy to each other. The thermal reaction of the model compounds reveal the following reaction mechanisms for 1,4 and 1,5-addition modes. Charges of atoms on the alkyne and azide group are shown in Figure 4.2. The three dimensional structure of the reactants, transition structures and products are shown in Figure 4.3.

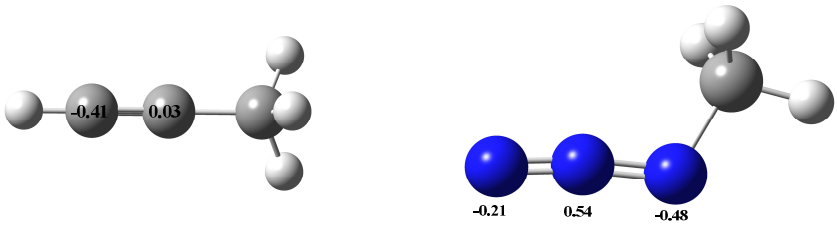

Figure 4.2 : Charges of atoms on the alkyne and azide groups (NBO charges).

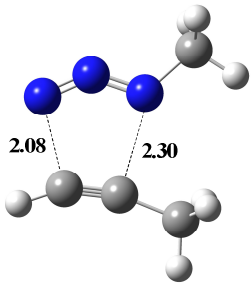

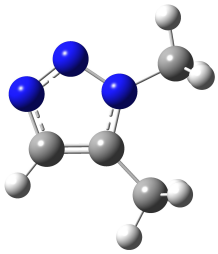

$TS_{1,5}$: 29.61 kcal/mol **1,5-triazole product:** -53.57 kcal/mol

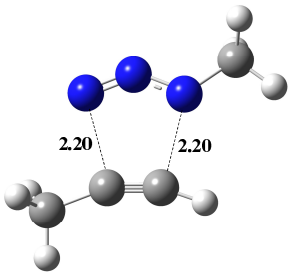

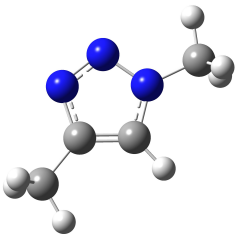

$TS_{1,4}$: 30.39 kcal/mol **1,4-triazole product:** -57.58 kcal/mol

Figure 4.3 : Transition states and products for the uncatalyzed model reaction.

The uncatalyzed reaction is concerted and bond formation is asynchronius in the case of 1,5-product formation. In the first type of attack, addition takes place by binding from the substituted nitrogen and carbon atoms via a transition state of 29.61 kcal/mol. In the second altenative, secondary nitrogen is bonding to the primary carbon atom via a transition state of 30.39 kcal/mol. The barriers to 1,4 and 1,5-cycloadditions are very close to each other, producing a mixture of experimentally observed regioisomeric products.

The uncatalyzed cycloaddition modes and their activation barriers are given which lead to 1,4 and 1,5-disubstituted products for entries model and 1 or 1,4,5 trisubstituted triazoles with the substitution on different carbon atoms for entries 2 and 3 (Figure 4.4 and Table 4.1).

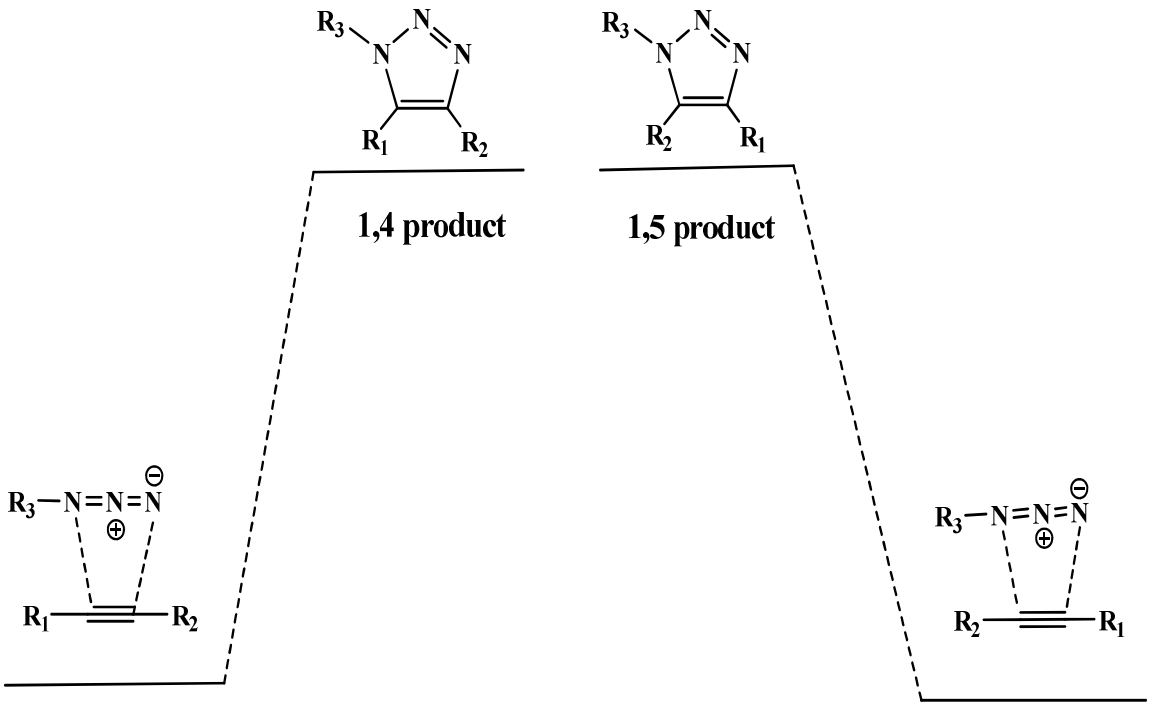

Figure 4.4 : Uncatalyzed addition modes of azide and alkyne with different substituents.

Table 4.1: Activation barriers of uncatalyzed azide-alkyne addition with different substituents.

entry	R1	R2	R3	Activation barrier for 1,4 product (kcal/mol)	Activation barrier for 1,5 product (kcal/mol)
Model	H	CH_3	CH_3	30.39	29.61
1	H	Ph	CH_2Ph	32.37	30.93
2	Ph	CH_2OH	CH_2Ph	35.05	31.29
3	Ph	COMe	CH_2Ph	31.14	32.45

Ruthenium Catalyzed:

At the first step of mechanism shown in Figure 4.1, spectator phospine ligands are displaced and a Ru-azide-alkyne complex is produced. This complex has been modeled and four possible structures have been obtained for this complex. These complexes for model reaction and their relative energies are shown in Figure 4.5.

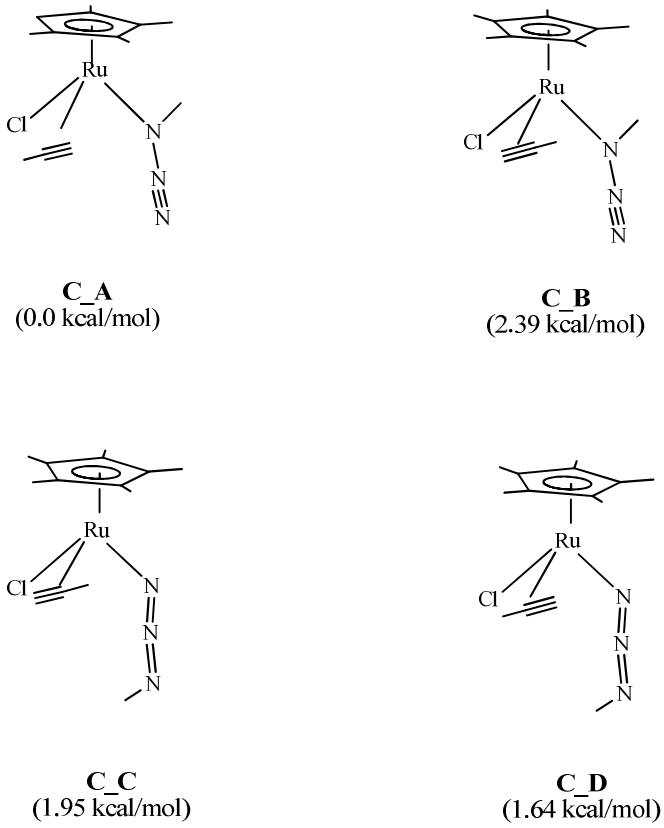

Figure 4.5 : Relative Electronic Energies of the Ru-alkyne-azide complexes

There are two sites for Ru to bind to the nitrogen atom: either from the secondary or from the primary nitrogen. In the work of Boren et al., the conformers that bond to the 2° nitrogen are more stable than the ones that bond to 1° nitrogen. It is stated in the literature that bonding can take from both sides, although bonding proximal to carbon is a more commonly observed bonding site [50]. The alkyne group can coordinate to the metal center in two orientations; methyl group directed towards the azide group or away from the azide group. The minimum structure was found to be structure C_A, where bonding is from the 2° nitrogen and the methyl group is directed away from the azide group so that the repulsive steric interactions are avoided. This is analogous to that of catalyst-azide-alkyne complex reported by Boren et al. where the structure of different configurations of methyl azide and propyne complexes with $CpRuCl(PPh_3)_2$ catalyst have been determined by B3LYP/6-31G* calculations. Reaction path shown in Figure 4.7 has been followed by taking C_A as the starting complex. The terminal nitrogen of azide group attacks the closest alkyne carbon via TSA_1 (shown in Figure 4.7). In this transition state

structure, Ru bonds more strongly to the unsaturated carbons; alkyne carbons open up towards a double bond length (1.255 Å in C_A and 1.292 Å in TSA_1) and the terminal carbon and the terminal nitrogen come closer (3.276 Å in C_A and 2.239 Å in TSA_1). As a result, an intermediate, named CA_1 is formed exothermically. The bond lengths generally do not change from C_A to CA_1 although in TSA_1 some bond lenghts dramatically change (such as increase in Ru-N bond length, decrease in Ru-alkyne bond length). In CA_1, the methyl group on alkyne is directed away from the Cp* ring and the metal center. The only steric repulsion is found between the methyl group on the azide and the methyl groups on the Cp* ring. After CA_1 forms, Ru metal will like to exempt from the cyclic structure. It can proceed via TSA_2 to form metal-triazole complex, CA_3. In CA_3, Ru stands out of the cycle and bonds to triazole from one of the nitrogen sides. The formation of Ru-triazole is highly exothermic. The triazole product will be formed by the regeneration of Ru catalyst.

An alternative reaction that can take after CA_1 is isomerization of this complex to a more stable six-membered ruthenacycle intermediate via TSA_3. This transformation takes place via a small free energy barrier of 2.24 kcal/mol. The forming ruthenacycle is 5.04 kcal/mol more stable than CA_1. In the literature, it is stated that "the facility and the outcome of the overall process are influenced by the relative energies and the ease of interconversion of intermediates CA_1 and CA_2"[22-23] . It is proposed that formation of CA_2 is disfavored in [Cp*RuCl] catalyzed reactions, thus, product formation is assumed to take place via TSA_2. In the literature, it is expected that the methyl groups on Cp* will cause great steric interactions with the azide and alkyne groups and in turn disable formation of a stable ruthenacycle. However, when the methyl groups are substituted on the cyclopentadiene ring in this study, the formation of the six-membered ring is facile and the reaction equilibrium may shift to CA_2 side due to 5.09 kcal/mol energy difference. It is seen that the relative energy of CA_2 is decreased with respect to its non-methylated analogue however, it is not high enough to prevent its formation. This intermediate has also been proposed in the experimental work of V.Fokin et al., where triazoles have been synthesized from internal alkynes in the presence of Ru catalyst. However, Ru-triazole complex formation via TSA_4 requires a 18.47 kcal/mol of barrier. Compared to the other path, this is a slower reaction since the rate-determining step via TSA_3 is 11.06 kcal/mol. Thus, intermediate CA_2 may

not be observed in the reaction. Critical bond distances of the structures in the C_A reaction coordinate are shown in Figure 4.6.

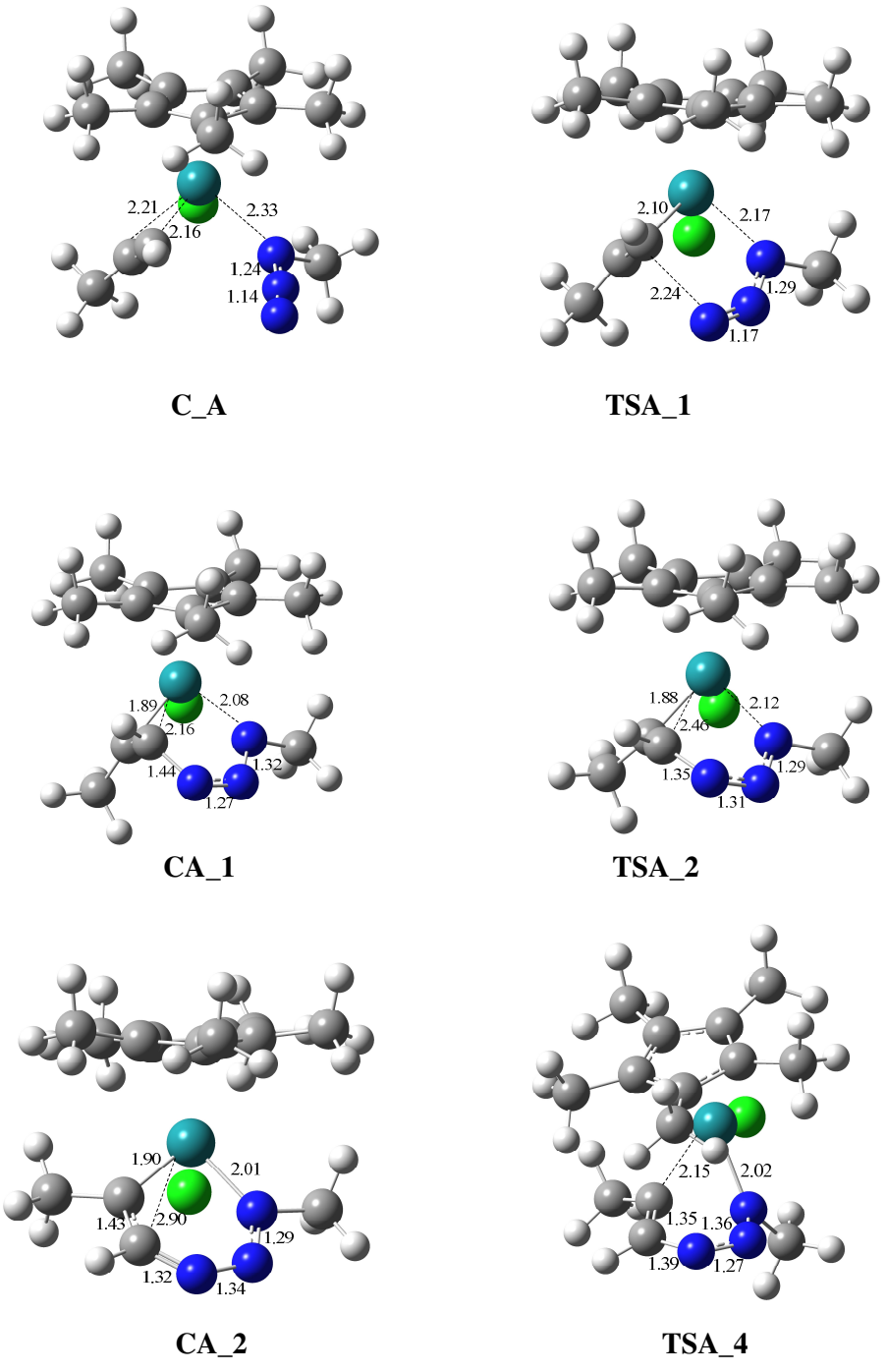

Figure 4.6 : Critical bond distances of the structuctures in the reaction coordinate starting from C_A.

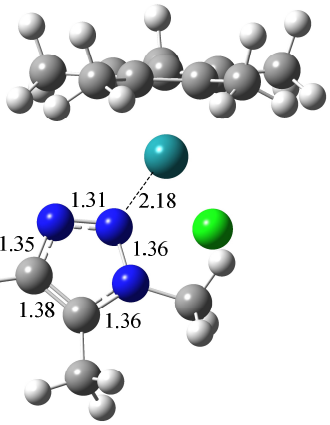

CA_4

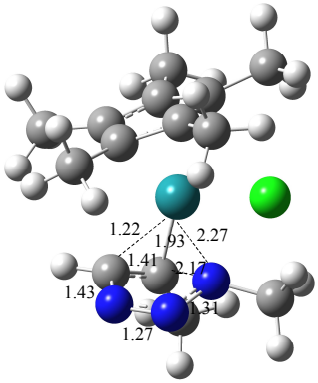

TSA_3

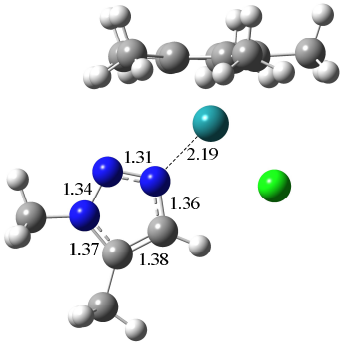

CA_3

Figure 4.6: (continued) Critical bond distances of the structuctures in the reaction coordinate starting from C_A.

In the C_B structure, Ru bonds to the 2° nitrogen of the azide. Methyl group on the alkyne is directing towards Ru and azide, so it has lower stability, compared to C_A (2.39 kcal/mol higher than C_A). The reaction mechanism starting with C_B is demonstrated in Figure 4.11. The reaction exibit a different sequence than that of C_A. In the reaction mechanism of C_A, CA_2 could be obtained via two steps, however, with C_B, the ruthenacycle intermediate could be obtained in a concerted fashion. The intermediate could be transformed to product through TSB_2, which yielded a 1,4-disubstituted product in an exothermic way. Although the reaction sequence is facile, the starting compound is higher than the global minimum which will not enable C_B to exist in the reaction medium. Following the same geometrical parameters of C_B for concerted addition of C_A did nor reveal a product. Critical bond distances of the structures in the C_B reaction coordinate are shown in Figure 4.8.

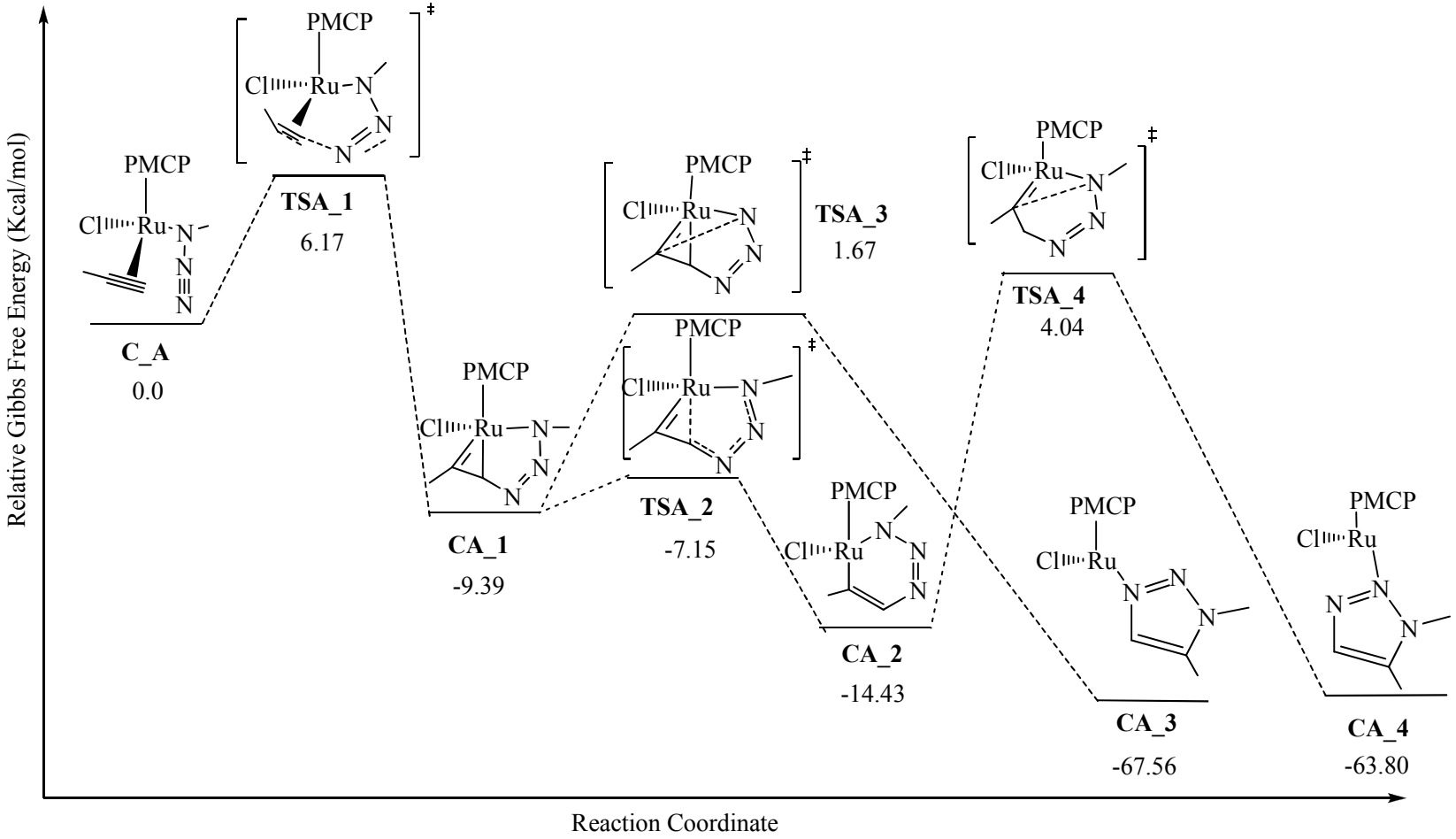

Figure 4.7 : Energetic profile for the Ru catalyzed model alkyne azide cycloaddition reaction starting from C_A

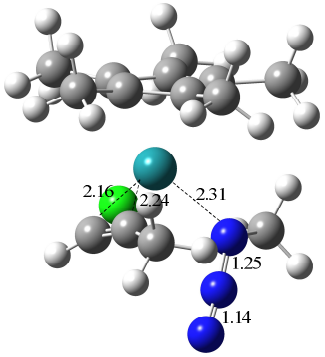

C_B

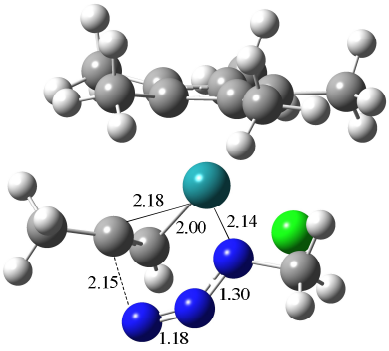

TSB_1

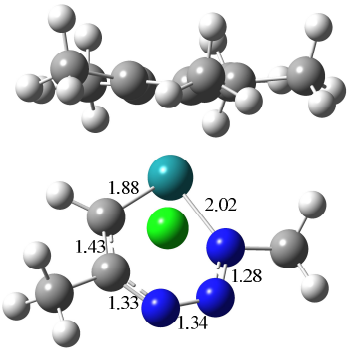

CB_1

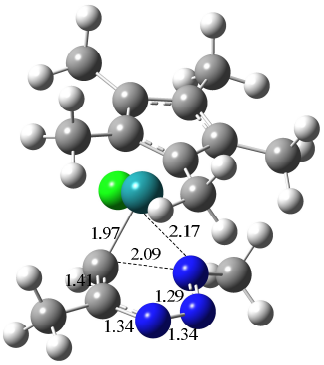

TSB_2

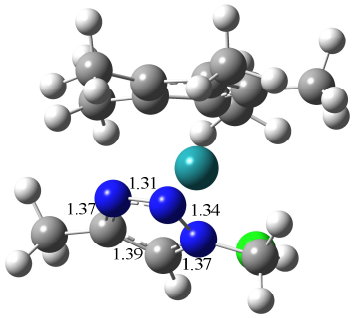

CB_2

Figure 4.8 : Critical bond distances of the structuctures in the reaction coordinate starting from C_B.

Relative electronic energies of C_C and C_D conformers are 1.95 and 1.64 kcal/mol, so they may be expected to survive in the reaction medium. C_C conformer would result in the formation of 1,5-regioisomer and C_D conformer would give 1,4-regioisomer. In the pathways (Figure 4.12), it is found out that the formation of the first intermediates has very high activation barriers; 22.01 kcal/mol and 17.01

kcal/mol. Critical bond distances of the structures in the C_C and C_D reaction coordinates are shown in Figure 4.9 and 4.10. Thus, we do not expect to have a product via these conformers, since the C_A structure is lower in energy and the rate determining step following C_A is lower in energy. According to Boltzmann distribution, the relative ratio, C_A : C_B: C_C : C_D, in the reaction medium is calculated as 89 : 2 : 3 : 6. Because of the fact that the amounts of C_C and C_D configurations are less than C_A and their activation barriers are very high as compared to that of C_A, it is not expected to have a product via these pathways.

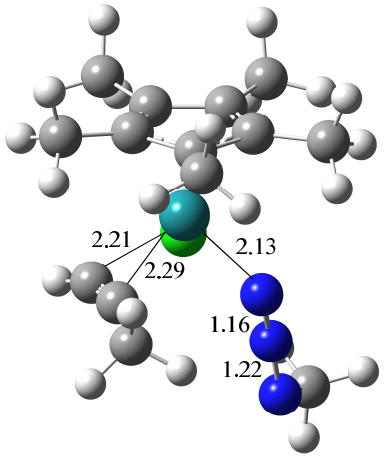

C_C

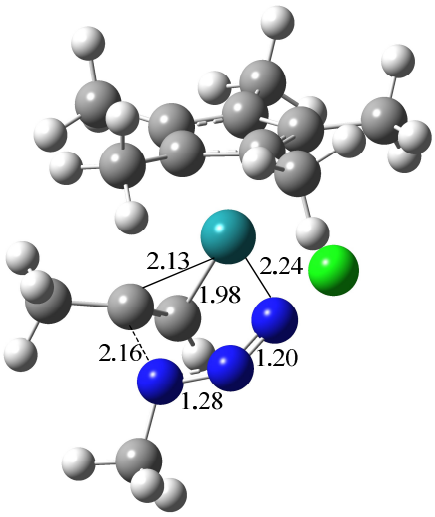

TSC_1

Figure 4.9 : Critical bond distances of the structuctures in the reaction coordinate starting from C_C.

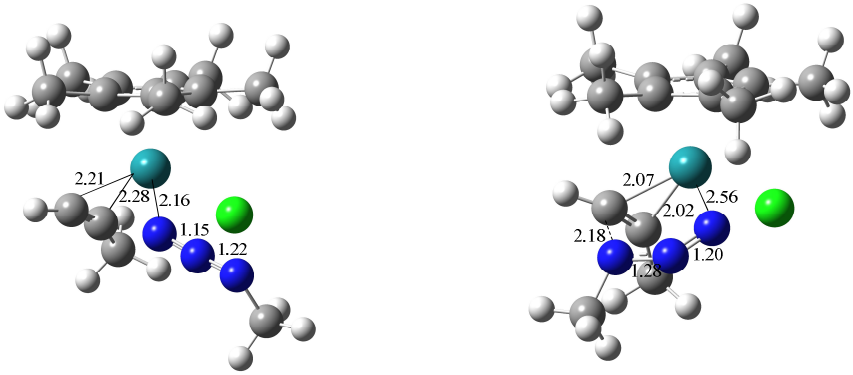

C_D **TSD_1**

Figure 4.10 : Critical bond distances of the structuctures in the reaction coordinate starting from C_D.

Compared to the uncatalyzed reaction of the model system, there is a dramatic change in the activation energies such that activation barrier for C_A in Ru catalyzed reaction is calculated as 6.17 kcal/mol, giving 1,5-triazole product whereas in the uncatalyzed case the reaction requires a barrier of 29.61 kcal/mol. The uncatalyzed reaction results giving a 1,4 - 1,5 triazole mixture despite of the 100:0 1,5-triazole regioselectivity of the Ru catalyzed process. These results are consistent with the formation of 1,4- and 1,5 mixture of products in the case of uncatalyzed reaction and regioselective and fast synthesis of 1,5-triazole with the Ru catalyst.

In the literature, the reaction between propyne and methyl azide with $[CpRuCl(PPh_3)_2]$ catalyst has been modeled [29]. The relative energies of their starting complexes are different than the relative energies of complexes with Cp* in sequence of C_A : C_B : C_C : C_D , 0.0 *(0.0)* : 0.8 *(2.39)* : 1.0 *(1.95)* : 0.7 *(1.64).* (The values in paranthesis refer to the relative energies in our study.) In these structures, the distance between Ru-N atoms are shorter, so, they bind more strongly. In addition to this, the rate determining steps of the configurations have higher barriers relatively 1-3 kcal/moles. The energies of C_A and the C_B complexes are closer to each other and their barriers are close thus with Cp ligand a product distribution is expected.

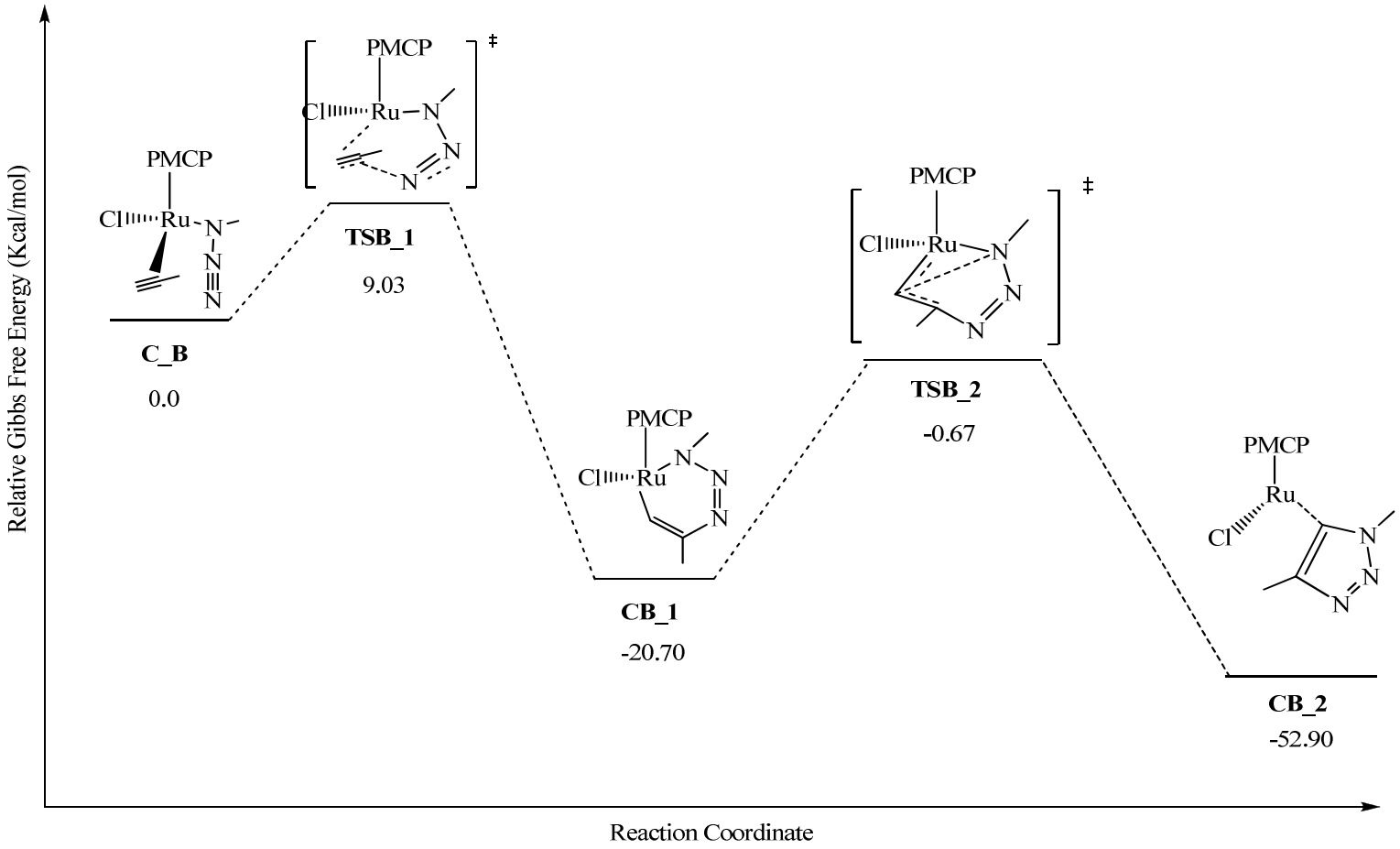

Figure 4.11 : Energetic profile for the Ru catalyzed model alkyne azide cycloaddition reaction starting from C_B.

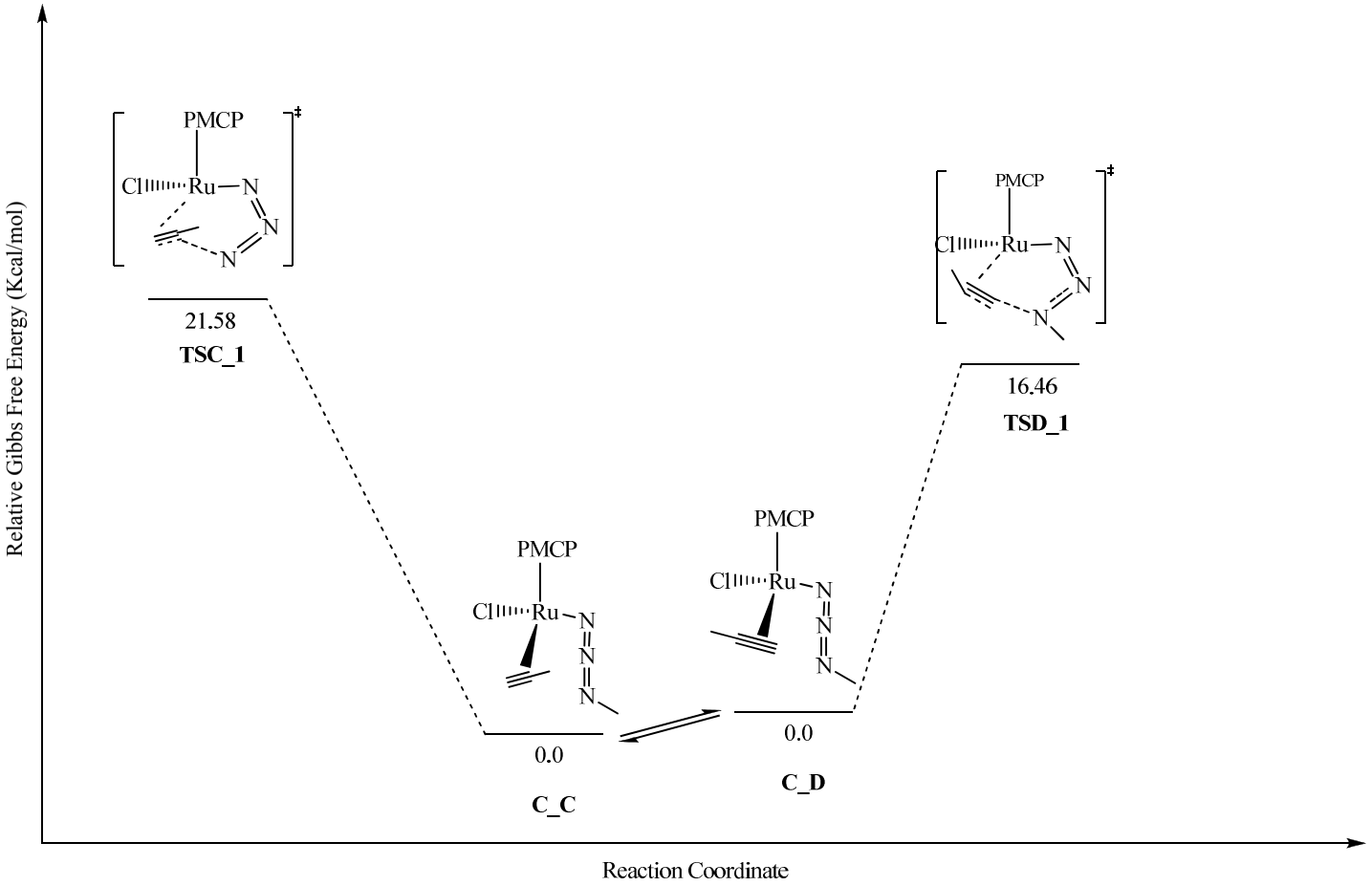

Figure 4.12 : Energetic profile for the Ru catalyzed model alkyne azide cycloaddition reaction starting from C_C and C_D.

4.2 Entry 1: The Reaction of Benzyl Azide and Phenyl Acethylene

At the second stage, a real system has been studied following the model reaction. In the real system, there is a phenyl group bonding to the alkyne, and a benzyl group bonding to the azide in the place of methyl groups. There are two sites for Ru to bond N, similiar to the model reaction; to the 2° nitrogen or to the 1° nitrogen.

According to the bonding sites for Ru to N, as in the model reaction case, four structures are obtained (Figure 4.13). In these four structures, the position of phenyl groups may vary and enable several conformers. As in the model case structure A has the lowest energy since it combines both the advantage of bonding from the secondary nitrogen of azide and the phenyl group being directed away from the steric hindrance.

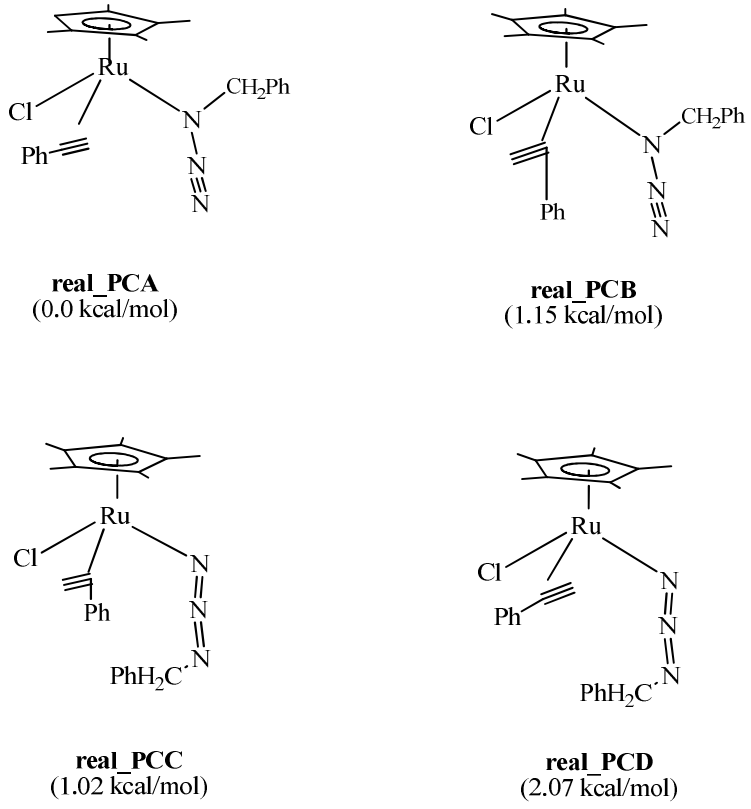

Figure 4.13 : Relative Electronic Energies of the complexes in the real system

Relative electronic energies for the real system structures are given below:

E_{C_A}= 0.0 kcal/mol E_{C_B}= 1.15 kcal/mol E_{C_C}= 1.02 kcal/mol E_{C_D}=2.07 kcal/mol

According to Boltzmann distribution, ratio of conformers in the reaction medium is as follows: C_A : C_B : C_C : C_D , 74 : 11 : 13 : 2.

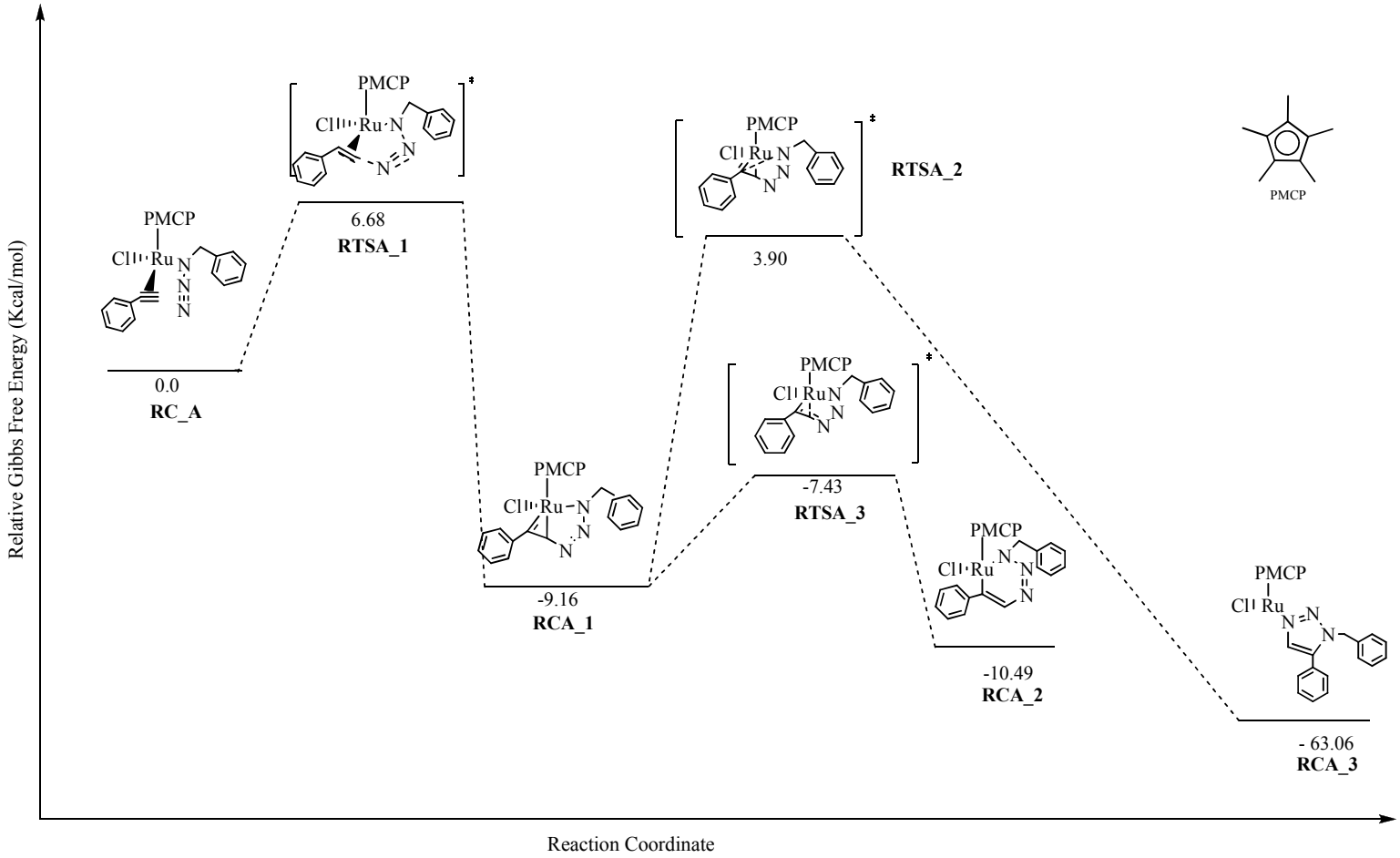

Figure 4.14 : Reaction path of RC_A conformer

In the reaction path of RC_A, shown in Figure 4.14, the starting complex RC_A, forms an intermediate RCA_1 exothermically via RTSA_1 transition state. In this stage, there are two ways for reaction to take place. First one is via RTSA_2 with an activation barrier of 13.06 kcal/mol through which RCA_3 is formed. In the second way, the reaction proceeds via transition state RTSA_3 with a small activation barrier of 1.73 kcal/mol. Then, a six-membered ruthenacycle intermediate is formed. It is proposed that, the steric interactions between Cp* and two phenyl groups will hinder the formation of a stable six-membered ruthenacycle intermediate[13]. Thus, it is stated in the literature that formation of the product is expected to proceed via RTSA_2.

In our calculations, the six membered intermediate is 1.3 kcal/mol more stable and its formation is favorable. However, formation of RCA_3 will hardly lead to product. In the model reaction, a transition state from six-membered intermediate was located 16.0 kcal/mol higher than CA_3. Thus, at least a 16 kcal/mol of barrier is also expected with the real case since a dramatic change in barriers has not been observed between the model and the real system. These results imply that the reaction mechanism may be via RTA_3.

Triazole formation via RC_B, RC_C and RC_D have also been considered, although their energies are much higher than RC_A. These mechanisms depicted in Figure 4.15 and 4.16. Substituents on alkyne and azide moietites have not made a significant change in barriers. Since their starting conformers are not stable enough compared to RC_A to exist in reaction medium, 1,4 or 1,5 product following RC_B, RC_C and RC_D are not expected. This result is in accordance with the literature. In the experimental study, only 1,5 triazoles were synthesized. According to our calculations, reaction mechanism starting from RC_A via TSA_2 is the most probable pathway.

4.2.1 Cp versus Cp*

As mentioned before, the reaction of benzylazide and phenylacetylene, called real system in this study, gives a mixture of 1,5 and 1,4 triazoles in 85:15 ratio by using Cp catalyst. The regioselectivity is determined by the nucleophilic attack of the alkyne group at the electrophilic terminal nitrogen of the azide which is called the oxidative coupling step. Firstly, the relative energies of the starting complexes are in a different manner compared to the structures with Cp* catalyst shown

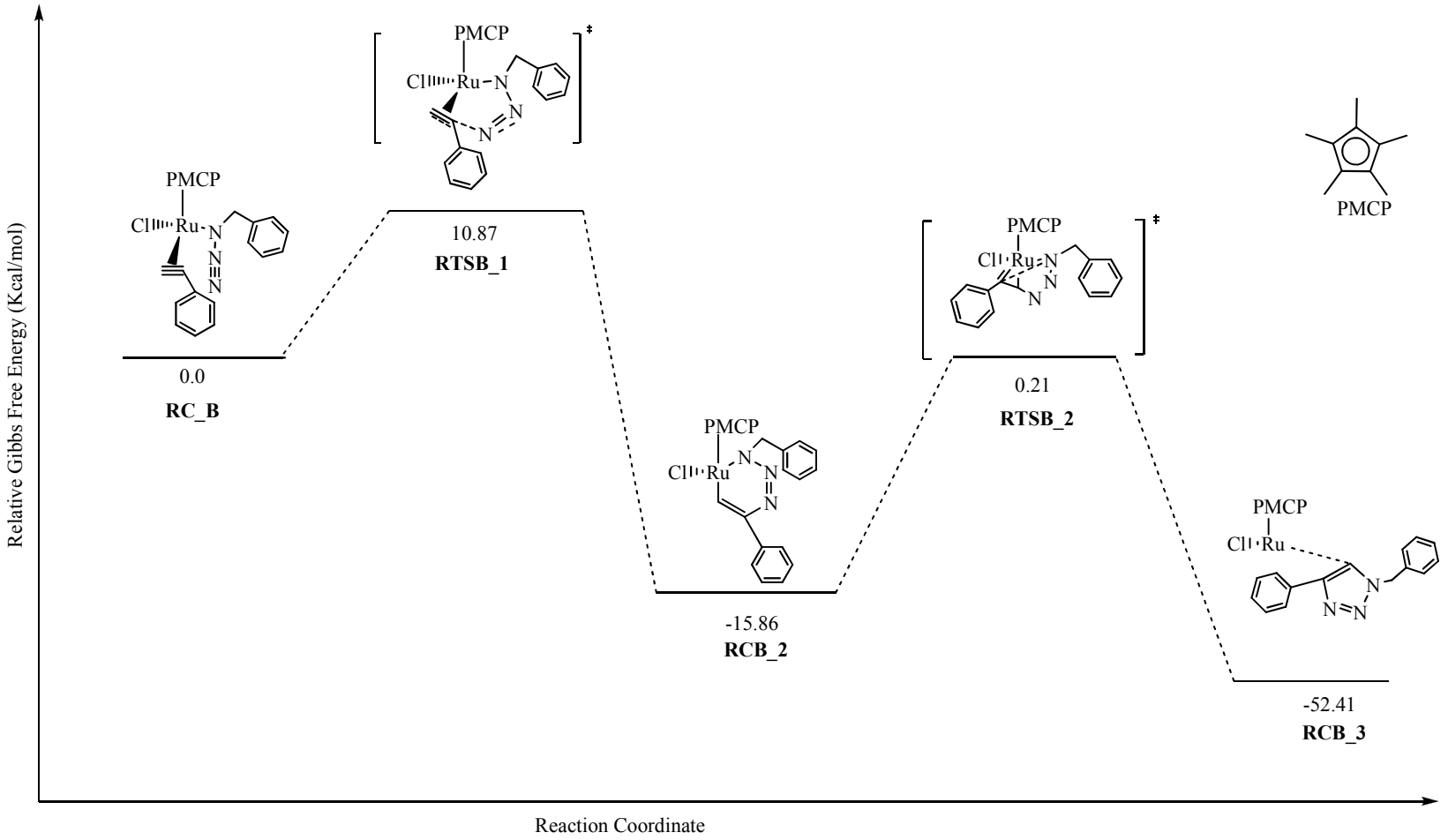

Figure 4.15 : Reaction path of RC_B conformer

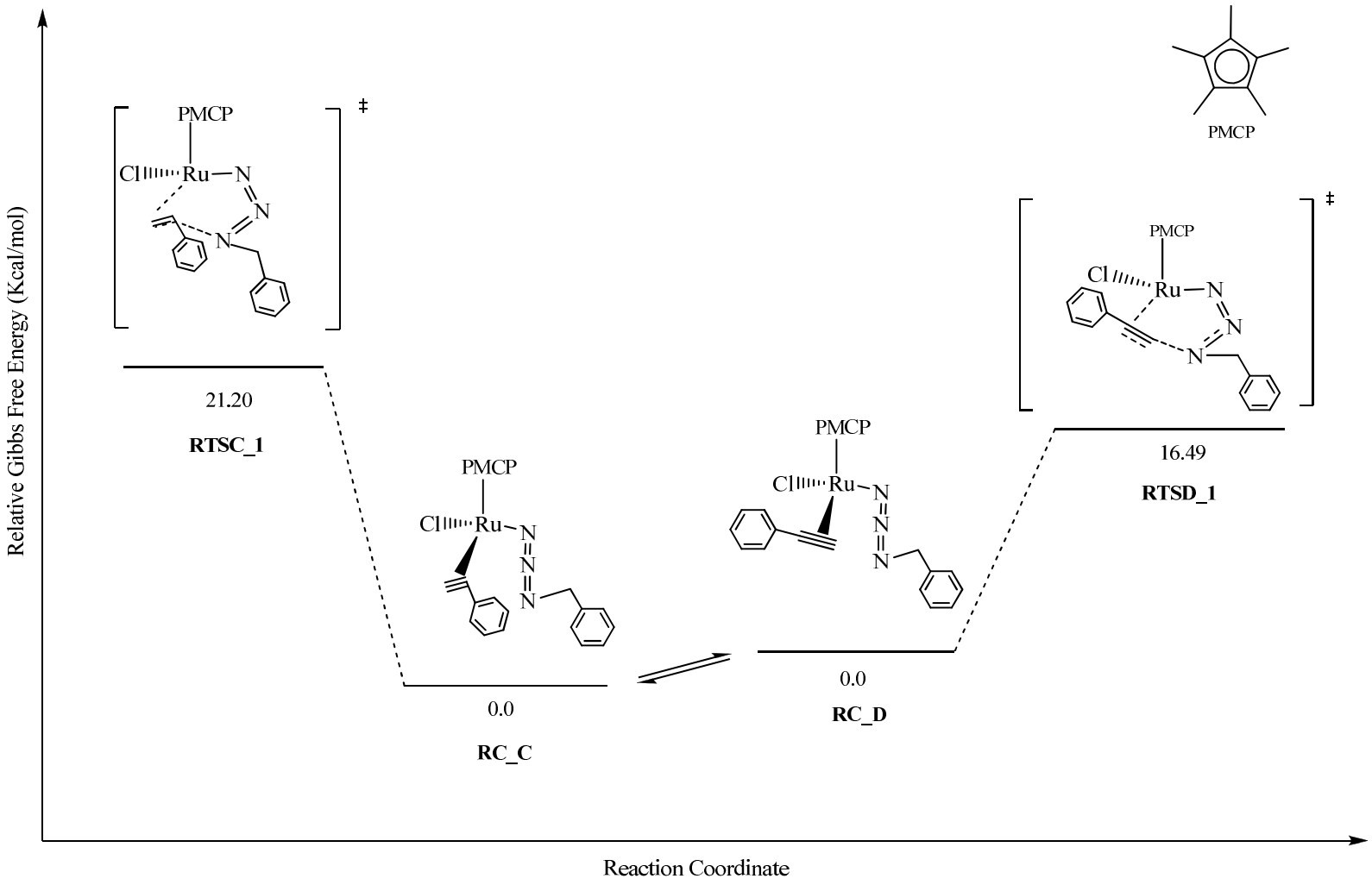

Figure 4.16 : Reaction paths of RC_C and RC_D conformers

in Figure 4.17. The minimum energy structure with the Cp catalyst is found to be the C_C configuration which leads to the 1,5-triazole. The following structure is C_B configuration with an energy of 0.34 kcal/mol and results giving a 1,4-triazole product.

In the reaction of benzylazide and phenylacetylene with Cp catalyst, the minimum structure is C_C, followed by C_B, C_A and C_D with energies of 0.13, 0.76, 2.52 kcal/moles.

According to Boltzmann distribution for these four structures, the ratio of configurations in the reaction medium is C_A : C_B : C_C : C_D , 13 : 38 : 48 : 1.

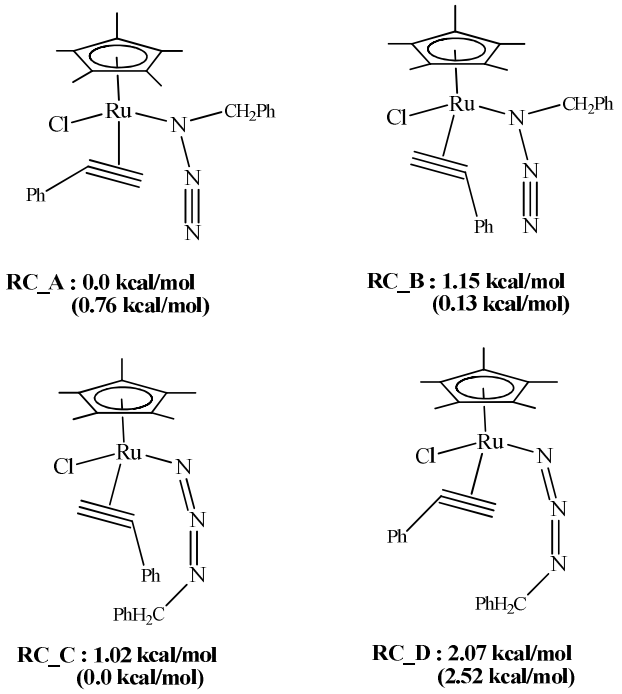

Figure 4.17 : Relative electronic energies of complexes with Cp and Cp* catalysts.(The values in paranthesis refer to the same complexes with cyclopentadienyl ligand on Ru.)

The activation barriers of first transition states for C_C and C_D structures are relatively high with 23.2 and 20.8 kcal/moles similar to the Cp* structures. In addition to this, their present ratio in the reaction medium is low, respectively. Thus, production of triazole is expected through the C_A and C_B structures. The rate-determining step of the C_A structure pathway has a barrier of 7.2 kcal/mol which results after several steps giving a 1,5-triazole.

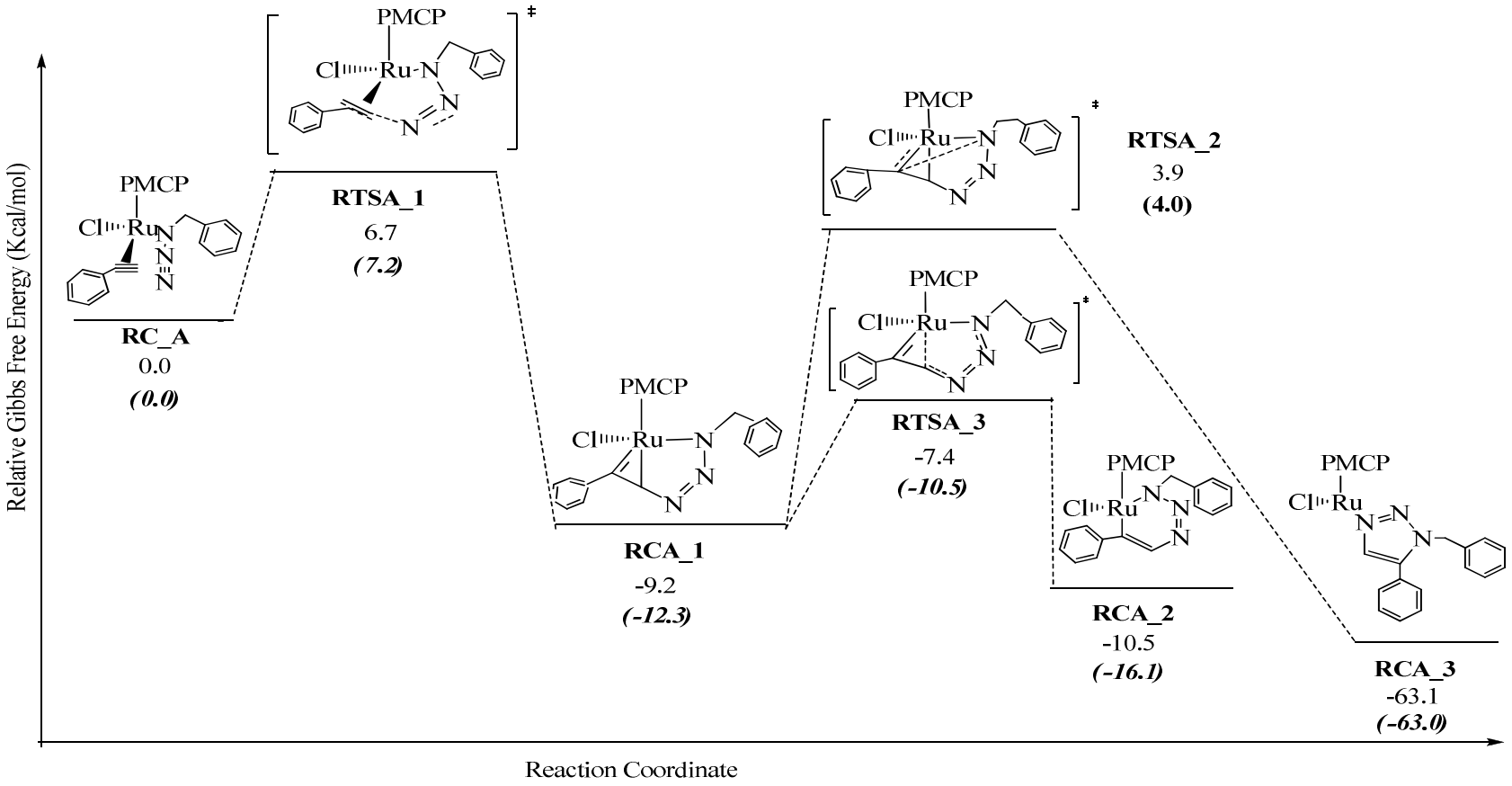

Figure 4.18 : Reaction path of RC_A configuration (The values in paranthesis refer to the same complexes with cyclopentadienyl ligand on Ru).

Considering the abundancy of C_A and its low barrier, this is the most favorable pathway. In the C_B configuration, there is still significant abundancy. Its activation barrier is 10.8 kcal/mol and it is competitive with the C_A structure.

The product distribution of 1,5:1,4-triazoles, 85:15 ratio can be attributed to the similar abundancy of the complexes (C_A and C_B) which lead to different regioselectivities.

4.3 Entries 2 and 3: Trisubstituted Triazoles

Two systems we discussed before are giving disubstituted triazoles. Entries 2 and 3 shown in Figure 4.21 are giving 1,4,5-trisubstituted triazoles. In these two reactions, internal alkynes are giving triazoles with a high regioselectivity, which is not possible by using the Cu catalyst.

Entry 2 is the reaction of 3-phenylprop-2-yn-1-ol with benzylazide. The product is A:B, 0:100 triazole with a yield of 70%. In entry 3 case, 100% product A is obtained starting from 4-phenylbut-3-yn-2-one and phenylazide. The main difference between 2 and 3 are the conformers with the minimum energy which lead to different products.

For entry 2, it is found that, PCA and PCC configurations lead to the experimentally obtained product. In the entry 3 case, product will be obtained via PCB and PCD configurations.

Relative electronic energies for entry 2 structures are given below:

E_{C_A}= 0.94 kcal/mol E_{C_B}= 6.47 kcal/mol E_{C_C}= 5.96 kcal/mol E_{C_D}= 0.0 kcal/mol

According to Boltzmann distribution it is found that, the ratio of present conformers in the reaction medium for entry 2 is C_A : C_B : C_C : C_D , 17 : 0 : 0 : 83. In this case, C_B and C_C conformers will not exist in the reaction.

The minimum structure for entry 2 was found to be structure C_D. The following minimum configuration is the C_A structure with energy 0.94 kcal/mol. In both structures, hydroxyl group on alkyne is directing towards to the chlorine atom. This interaction provides stabilization in these two structures. On the other hand, the hydroxyl groups on C_B and C_C are directing to the azide. This interaction decreases the reactivity of the azide group, therefore they have higher energies relatively.

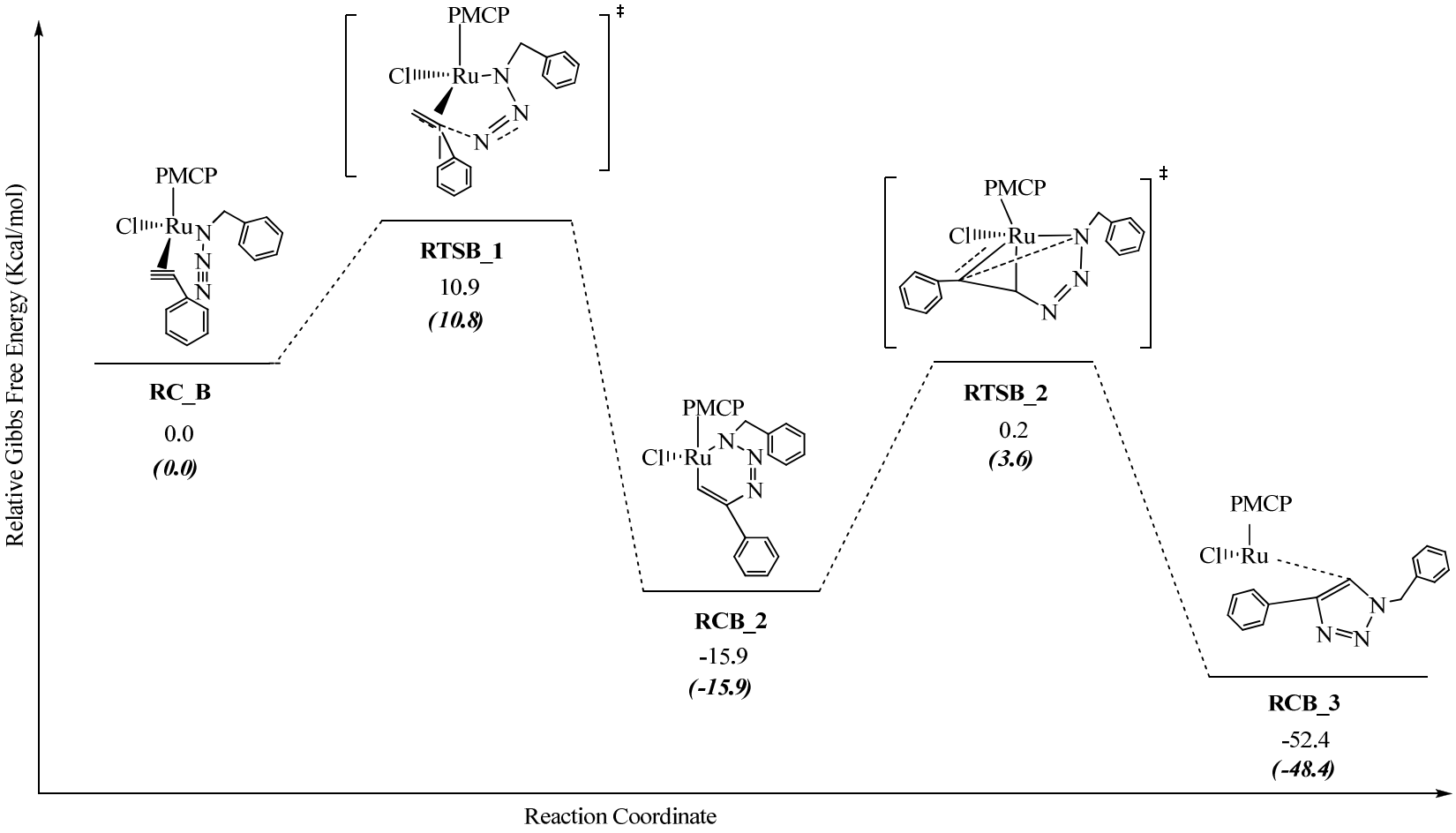

Figure 4.19 : Reaction path of RC_B configuration (The values in paranthesis refer to the same complexes with cyclopentadienyl ligand on Ru.)

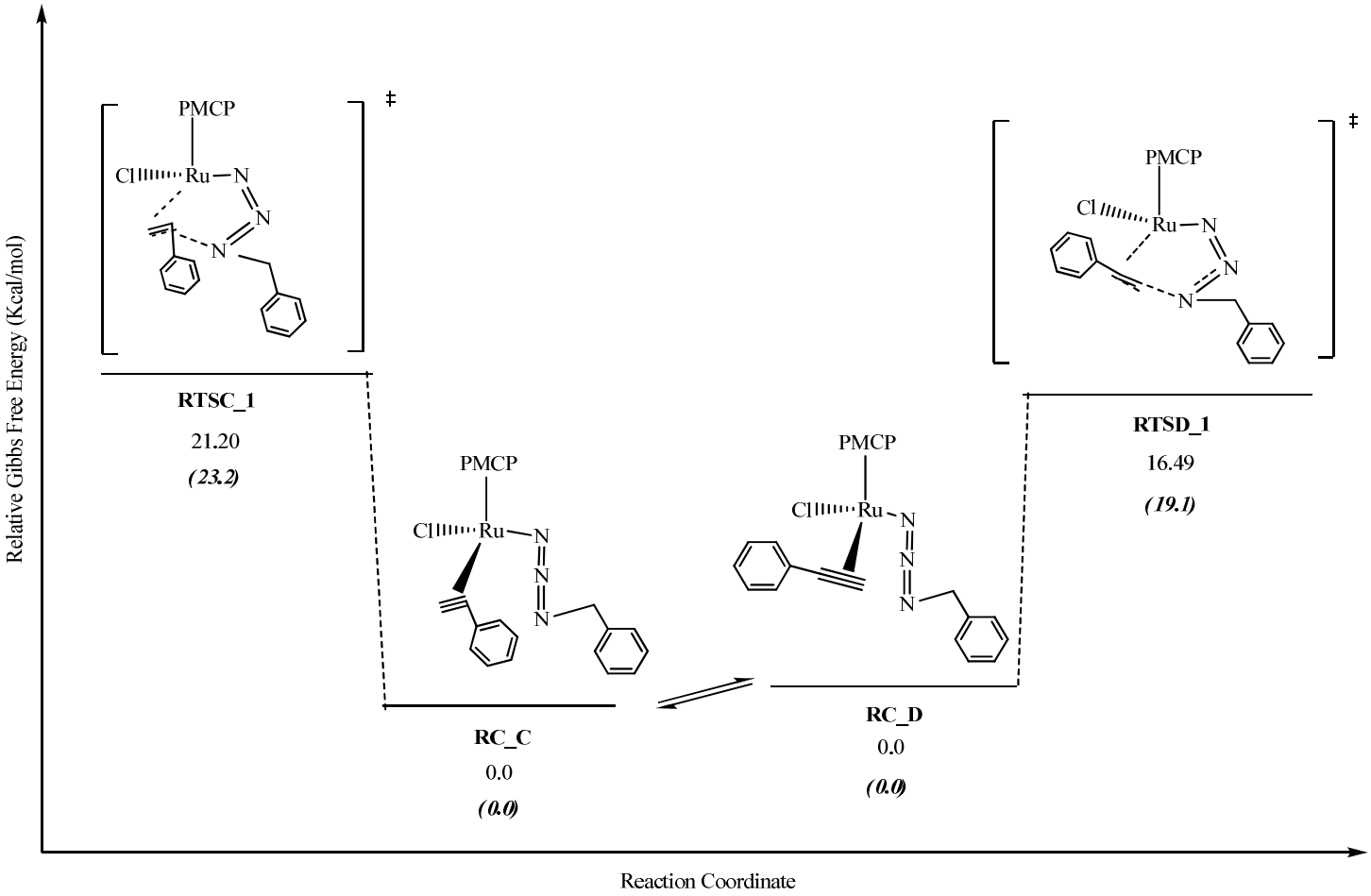

Figure 4.20 : Reaction path of RC_C and RC_D configurations (The values in paranthesis refer to the same complexes with cyclopentadienyl ligand on Ru.)

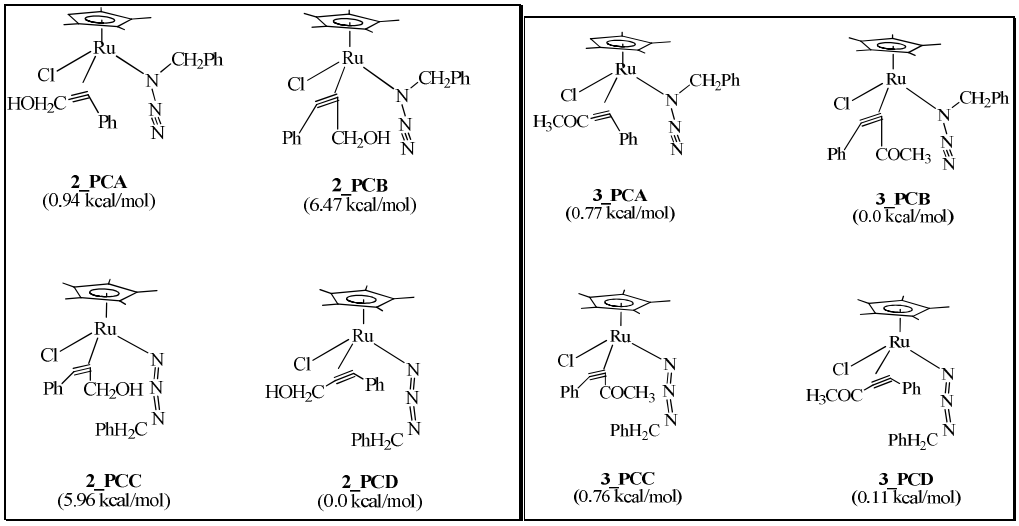

Figure 4.21 : Relative Electronic Energies of the Ru-alkyne-azide complexes for entries 2 - 3.

The terminal nitrogen of azide group attacks to the closest alkyne carbon via TSA_1. As a result, CA_2 intermediate is formed via a transition state of 10.12 kcal/mol. Via TSA_4, this intermediate turns into a 1,4,5-trisubstituted triazole. In product CA_4, Ru stands out of the cycle and bonds to triazole from one of the nitrogen sides. The formation of Ru-triazole is highly exothermic with an energy of 52.78 kcal/mol.

Starting conformer of C_B has an energy of 6.47 kcal/mol and the presence of this complex is very low in the reaction medium. Methylhydroxyl group on the alkyne increases the reactivity of the carbon atom of the triple bond, therefore the barrier of TSB_1 is lower than that of TSA_1. Although C_B has a low transition state energy of 5.17 kcal/mol, it is not expected to have a product via this conformer because the starting structure will not exist in the reaction medium.

Relative electronic energies of C_C and C_D conformers are 5.96 and 0.0 kcal/moles. C_C conformer would result in the formation of B type and C_D conformer would give A type of product. In the pathways of C_C and C_D, it is found out that the formations of the first intermediates have very high activation barriers, 20.42 kcal/mol and 23.56 kcal/mol. Whatever their starting energies are, we do not expect to have a product via these conformers because of their high TS barriers.

As a result, product will be formed via C_A configuration which has a 17% abundancy in the reaction medium. 70% yield of this reaction could be attributed to the low amount of this complex giving product.

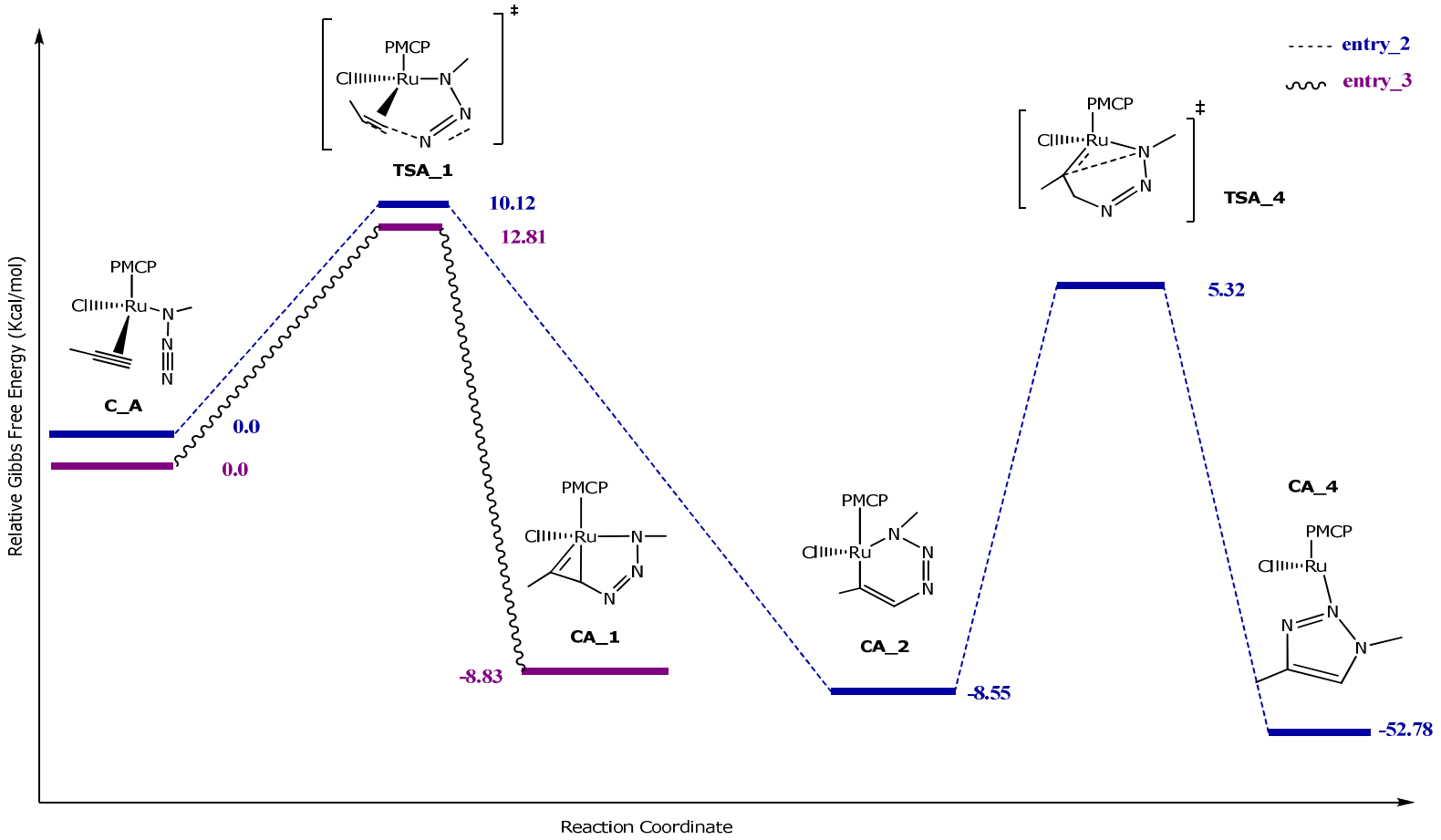

Figure 4.22 : Energetic profile for the Ru catalyzed alkyne azide cycloaddition reaction of entries 2 and 3 starting from **C_A.**

In entry 3, the minimum structure configuration is C_B, followed by C_D, C_C and C_A with relative energies of 0.11, 0.76, 0.77 kcal/moles.

According to Boltzmann distribution for entry 3, ratio of conformers in the reaction medium is 11 : 42 : 12 : 35 for C_A : C_B : C_C : C_D.

The minimum structure for entry 3 was found to be structure C_B. The following minimum configuration is the C_D structure with energy 0.11 kcal/mol.

The terminal nitrogen of azide group attacks to the closest alkyne carbon via TSB_1 with an energy barrier of 9.75 kcal/mol and CB_2 intermediate is formed. Via TSB_3, this intermediate turns into a 1,4,5-trisubstituted triazole. CB_3 product formation of Ru-triazole is highly exothermic with an energy of 57.10 kcal/mol and gives B type product..

Starting transition state of C_A has an energy of 12.81 kcal/mol and this barrier is higher as compared to TSB_1. In addition to this, the ratio of C_A is lower than C_B configuration with a relatively high barrier.

Relative electronic energies of C_C and C_D conformers are 0.76 and 0.11 kcal/moles. In both configurations, the reaction begins with the attack of the secondary nitrogen to the alkyne group. The activation barriers of the first transition states are found as 26.15 and 25.06 kcal/moles which are relatively high as compared to the rate determining steps of the C_A and C_B structures which enables to have a product via these configurations.

C_B and C_D configurations will result giving A type product, which is experimentally observed. As a result, product will be formed via C_B configuration which has a 42% abundancy in the reaction medium. 35% C_D structure abundancy will not give any product because of its high activation barrier.

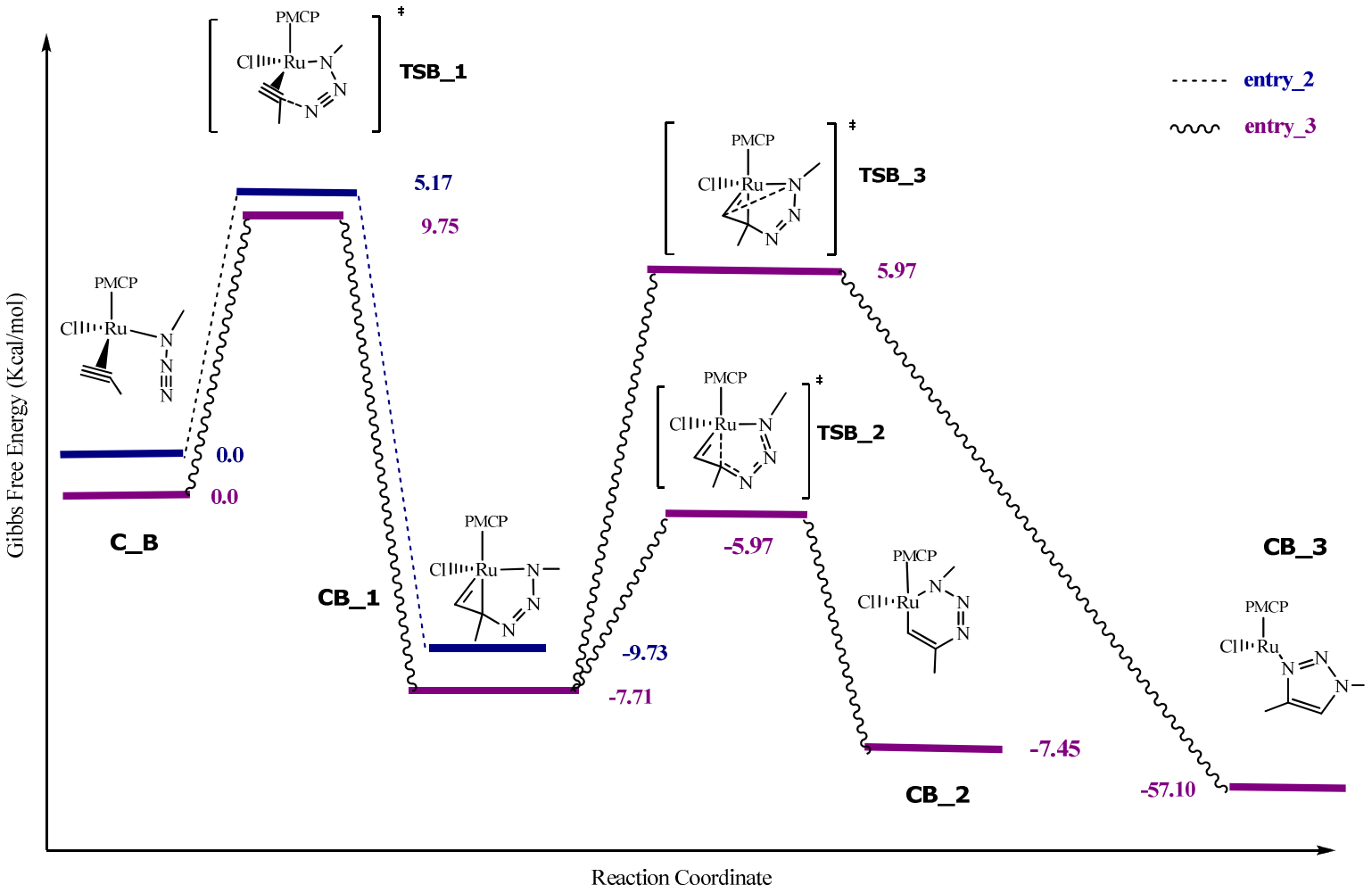

Figure 4.23 : Energetic profile for the Ru catalyzed alkyne azide cycloaddition reaction of entries 2 and 3 starting from C_B

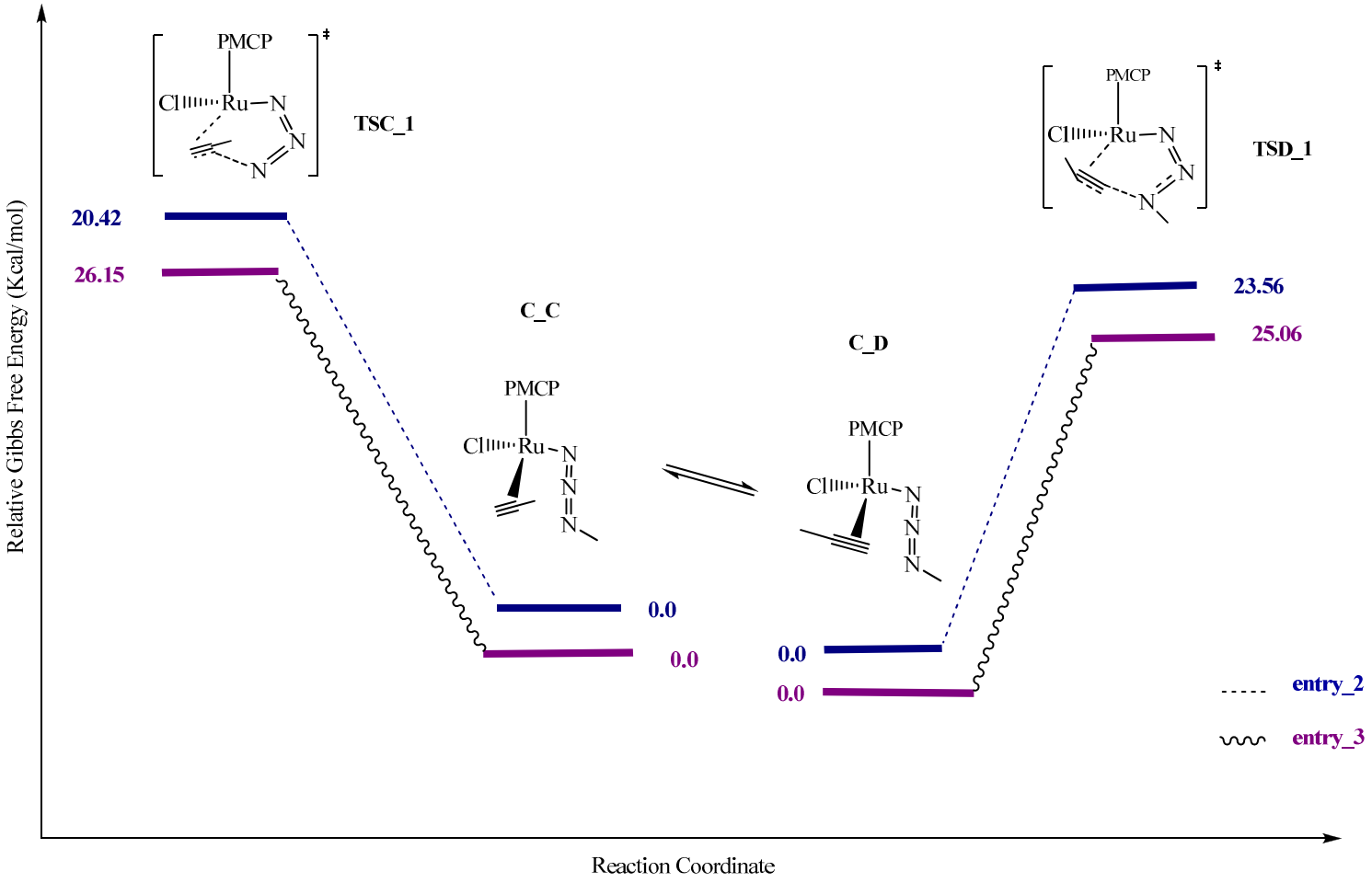

Figure 4.24 : Energetic profile for the Ru catalyzed alkyne azide cycloaddition reaction of entries 2 and 3 starting from C_C and C_D

5. CONCLUSION

In this study, a ruthenium catalyzed azide-alkyne cycloaddition reaction has been modeled by quantum mechanical methods. In the first part of the study, a model reaction has been analyzed. This model reaction has served to establish basic facts about the mechanism of the reaction mentioned. According to this model, at the first step of mechanism, spectator ligands are displaced and a Ru-azide-alkyne complex is produced. This complex rearranges. Two different intermediates have been proposed in two different studies in the literature. In the model study, the 6-membered cyclic intermediate has been discarded since the reaction after this intermediate is calculated to be energetically unfavored compared to the other alternative. Although the relative stability of CA_1 and CA_2 have been considered as the driving force of the reaction in previous work, in this study reaction following this intermediate has been unfacile. In the previous study cyclopentadiene was lacking methyl groups and the methyl groups were expected to be stabilizing the 6-membered intermediate. However, no such difference has been found in this study. Calculations on the reactants of entry 1 have changed the steric interactions, however, the general trend has not been changed by the phenyl groups. The same mechanism is calculated to be the facile pathway.

The Ru-azide-alkyne complexes (C_A, C_B, C_C, C_D) can lead to 1,4 or 1,5-triazole products. The experimental 100% 1,5-triazole formation when Cp is methylated is verified by the calculations on real system.

In entry 2 and 3 case, the reaction of azide with internal alkynes has been investigated. As an outcome of these reactions, 1,4,5 trisubstituted triazoles are obtained. Similarly, the relative energies of the starting complexes and their first activation barriers are effective to determine the product distribution. C_C and C_D structures for both entries have high activation barriers, therefore the product will be derived from the C_A and C_B configurations.

REFERENCES

[1] **Tome´, A. C.,** 2004: in Science of Synthesis: Houben-Weyl Methods of Molecular Transformations: *Five-Membered Hetarenes with Three or More Heteroatoms*, vol. **13**, pp. 415–601 ed. R. C. Storr and T. L. Gilchrist, Thieme, Stuttgart.

[2] **Krivopalov, V. P. and Shkurko, O. P.,** 2005: 1,2,3-Triazole and its derivatives. Development of methods for the formation of the triazole ring, *Russian Chemical Reviews*, **74**, 339–379.

[3] **Grana, G.,** 2006: Adjuvant aromatase inhibitor therapy for early breast cancer: A review of the most recent data, *Journal of Surgical Oncology*, **7**, 586-592.

[4] **Chao, S., Oh, S., Um, Y. Jung, J. H., Ham, J., Shin, W. S. and Lee, S.,** 2009: Synthesis of 10-substituted triazolyl artemisinins possessing anticancer activity via Huisgen 1,3-dipolar cylcoaddition, *Bioorganic and Medicinal Chemistry Letters,* **19**, 382-385.

[5] **Zhang, J.-J., Garrossian, M., Gardner, D., Garrossian, A., Chang, Y.-T., Kim, Y. K. and Tom Chang, C.,** 2008: Synthesis and anticancer activity studies of cyclopamine derivatives, *Bioorganic and Medicinal Chemistry Letters*, 18, 1359-1363.

[6] **Odlo, K.; Hentzen, J.; dit Chabert, J. F., Ducki, S., Gani, O. A. B. S. M., Sylte, I., Skerede, M., Flørenes, V. A. and Hansen, T. V.,** 2008: 1,5-Disubstituted 1,2,3-triazoles as *cis*-restricted analogues of combretastatin A-4: Synthesis, molecular modeling and evaluation as cytotoxic agents and inhibitors of tubulin, *Bioorganic and Medicinal Chemistry*, **16**, 4829-4838.

[7] **Alvarez, R., Velazquez, S., San, F., Aquaro, S., De, C., Perno, C. F., Karlsson, A., Balzarini, J. and Camarasa, M. J.,** 1994: 1,2,3-Triazole-[2,5-Bis-O-(tert-butyldimethylsilyl)-.beta.-D-ribofuranosyl]-3'-spiro-5"-(4"-amino-1",2"-oxathiole 2",2"-dioxide) (TSAO) Analogs: Synthesis and Anti-HIV-1 Activity, *Journal of Medicinal Chemistry*, **37**, 4185-4194.

[8] **da Silva, F., de, C., de Souza, C. B. V., Frugulhetti, I. I. P., Castro, H. C., Souza, A. M. T., Abreu, P. A., Passamani, F., Rodrigues, C. R. and Ferreira, V. F.,** 2009: Synthesis, HIV-RT inhibitory activity and SAR of 1-benzyl-1*H*-1,2,3-triazole derivatives of carbohydrates, *European Journal of Medicinal Chemistry*, **44**, 373-383.

[9] **Buckle, D. R., Rockell, C. J. M., Smith, H. and Spicer, B. A.,** 1986: Studies on 1,2,3-triazoles. 13. (Piperazinylalkoxy)-[1]benzopyrano[2,3-d]-1,2,3-triazol-9(1H)-ones with combined H1-antihistamine and mast

cell stabilizing properties, *Journal of Medicinal Chemistry*, **29**, 2262-2267.

[10] **Joan, C. F. T., Elizabeth, H., Beatrice, M. and Daniel, P. B.,** 1998: In Vitro Activity of a New Oral Triazole, *Antimicrobial Agents and Chemotherapy*, **42**, 313-318.

[11] **Genin, M. J., Allwine, D. A., Anderson, D. J., Barbachyn, M. R., Emmert, D. E., Garmon, S. A., Graber, D. R., Grega, K. C., Hester, J. B., Hutchinson, D. K., Morris, J., Reischer, R. J., Ford, C. W., Zurenko, G. E., Hamel, J. C., Schaadt, R. D., Stapert, D. and Yagi, B. H.,** 2000: Substituent Effects on the Antibacterial Activity of Nitrogen–Carbon-Linked (Azolylphenyl)oxazolidinones with Expanded Activity Against the Fastidious Gram-Negative Organisms Haemophilus influenzae and Moraxella catarrhalis, *Journal of Medicinal Chemistry,* **43**, 953-970.

[12] **Périon, R., Ferrières, V., García- Moreno, M. I., Mellet, C. O., Duval, R., Fernández, J. M. G. and Plusquellec, D.,** 2005: 1,2,3-Triazoles and related glycoconjugates as new glycosidase inhibitors, *Tetrahedron,* **61,** 9118-9128.

[13] **Shen, J., Woodward, R., Kedenburg, J. P., Liu, X.-W., Chen, M., Fang, L.-Y., Sun, D.-X. and Wang, P.-G.,** 2009: Histone Deacetylase Inhibitors through Click Chemistry, *Journal of Medicinal Chemistry,* **51**, 7417-7427.

[14] **Hou, D.-R., Alam, S., Kuan, T. C., Ramanathan, M., Lin, T.-P. and Huang, M.-S.,** 2009: 1,2,3-Triazole derivatives as new cannabinoid CB1 receptor antagonists, *Bioorganic and Medicinal Chemistry Letters*, **19**, 1022-1025.

[15] **Jordã, A. K., Ferreira, V. F., Lima, E. S., de Souza, M. C. B. V., Carlos, E. C. L., Castro, H. C., Geraldo, R. B., Rodrigues, C. R., Almeida, M. C. B. and Cunha, A. C.,** 2009: Synthesis, antiplatelet and in silico evaluations of novel N-substituted-phenylamino-5-methyl-1*H*-1,2,3-triazole-4-carbohydrazides, *Bioorganic and Medicinal Chemistry,* **17**, 3713-3719.

[16] **Thompson, A. M., Blaser, A., Anderson, R. F., Shinde, S. S., Franzblau, S. G., Ma, Z.-K., Denny, W. A. and Palmer, B. D.,** 2009: Synthesis, Reduction Potentials, and Antitubercular Activity of Ring A/B Analogues of the Bioreductive Drug (6S)-2-Nitro-6-{[4-(trifluoromethoxy)benzyl]oxy}-6,7-dihydro-5H-imidazo[2,1b][1,3] oxazine, *Journal of Medicinal Chemistry,* **52,** 637-645.

[17] **Hoshino, M.,** 1960: Effect of 3-Amino-1,2,4-triazole on the Experimental Production of Liver Cancer, *Nature*, **186**, 174-175.

[18] **Guo, L., Li, Z., Wang, H. and Zhang, C. Ye, D.,** 2006: Carboxyamido-triazole inhibits proliferation of human breast cancer cells via G_2/M cell cycle arrest and apoptosis, *European Journal of Pharmacology*, **538,** 15-22.

[19] **Rashad, A. E., El-Sayed, W. A., Mohamed, A. M. and M. M. Ali,** 2010: Synthesis of New Quinoline Derivatives as Inhibitors of Human Tumor Cells Growth, *Archiv der Pharmazie - Chemistry* in *Life Sciences,* **8**, 440-448.

[20] **Wasilenko, W. J., Palad, A. J., Sommers, K. D., Blackmore, P. F., Kohn, E. C., Rhim, J. S., Wright, G. L., and P. F. Schellhammer, J.R,** 1996:

Effects of the calcium influx inhibitor carboxyamido-triazole on the proliferation and invasiveness of human prostate tumor cell lines, *International Journal of Cancer*, **68,** 259-264.

[21] **Huisgen, R.,** 1984: in *1,3-Dipolar Cycloadditional Chemistry*, Ed.: A. Padwa, Wiley, New York.

[22] **Gothelf, K. V., and Jorgensen, K. A.,** 1998: A review of asymmetric 1,3-dipolar cycloaddition reactions, *Chemical Reviews*, **98,** 863-909.

[23] **Mulzer, J.,** 1991: A review of synthetic applications, *Organic Synthesis Highlights,* 77–95.

[24] **Katritzky, A. R., and Singh, S. K.,** 2002: Synthesis of C-Carbamoyl-1,2,3-triazoles by Microwave-Induced 1,3-Dipolar Cycloaddition of Organic Azides to Acetylenic Amides, *Journal of Organic Chemistry*, **67,** 9077-9079.

[25] **Wang, Z.-X., and Qin, H.-L.,** 2003: Regioselective synthesis of 1,2,3-triazole derivatives via 1,3-dipolar cycloaddition reactions in water, *Chemical Communications,* 2450-2451.

[26] **Harju, K., Vahermo, M., Mutikainen, I., and Yli-Kauhaluoma, J.,** 2003: Solid-Phase Synthesis of 1,2,3-Triazoles via 1,3-Dipolar Cycloaddition, *Journal of Combinatorial Chemistry,* **5**, 826-833.

[27] **Molteni, G., and Ponti, A.,** 2003: Arylazide Cycloaddition to Methyl Propiolate: DFT-Based Quantitative Prediction of Regioselectivity, *Chemistry – A European Journal,* **9,** 2770-2774.

[28] **Akritopoulou-Zanze, I., Gracias, V., and Djuric, S. W.,** 2004: A versatile synthesis of fused triazolo derivatives by sequential Ugi/alkyne-azide cycloaddition reactions, *Tetrahedron Letters*, **45,** 8439-8441.

[29] **Boren, B.C., Narayan, S., Rasmussen ,L. K., Zhang, L., Zhao, H., Lin, Z., Jia, G., and Fokin, V. V.,** 2008: Ruthenium-Catalyzed Azide−Alkyne Cycloaddition: Scope and Mechanism, *Journal of American Chemical Society,* **130,** 8923-8930.

[30] **Bastide, J., and Henri-Rousseau, O.,** 1973, *Bulletin de la Societe Chimique de France,* 2294-2296.

[31] **Clarke, D., Mares, R. W., and McNab, H.,** 1997: Preparation and pyrolysis of 1-(pyrazol-5-yl)-1,2,3-triazoles andrelated compounds, *Journal of the Chemical Society, Perkin Transactions 1,* 1799-1804.

[32] **Kolb, H. C., Finn M. G., and Sharpless, K. B.,** 2001: Click Chemistry: Diverse Chemical Function from a Few Good Reactions, *Angewandte Chemie International Edition*, **40**, 2004-2021.

[33] **Rostovtsev, V. V., Green, L. G., Fokin, V. V., and Sharpless, K. B**., 2002: A Stepwise Huisgen Cycloaddition Process: Copper(I)-Catalyzed Regioselective "Ligation" of Azides and Terminal Alkynes, *Angewandte Chemie International Edition*, **41**, 2596-2599.

[34] **Tornøe, C. W., Christensen, C., and Meldal, M.,** 2002: Peptidotriazoles on Solid Phase: [1,2,3]-Triazoles by Regiospecific Copper(I)-Catalyzed

1,3-Dipolar Cycloadditions of Terminal Alkynes to Azides, *Journal of Organic Chemistry,* **67**, 3057-3064.

[35] **Appukkuttan, P., Dehaen, W., Fokin, V. V., and van der Eycken, E.,** 2004: A Microwave-Assisted Click Chemistry Synthesis of 1,4-Disubstituted 1,2,3-Triazoles via a Copper(I)-Catalyzed Three-Component Reaction, *Organic Letters*, **6,** 4223-4225.

[36] **Hein J. E., and Fokin, V. V.,** 2010: Copper-catalyzed azide–alkynecycloaddition (CuAAC) and beyond: new reactivity of copper(I) acetylides, *Chemical Society Reviews*, **39**, 1302-1315.

[37] **Bock, V. D., Hiemstra, H., and. van Maarseveen, J. H**., 2006: Cu(I)-Catalyzed Alkyne–Azide "Click" Cycloadditions from a Mechanistic and Synthetic Perspective, *European Journal of Organic Chemistry,* 51-68.

[38] **Zhang, L., Chen, X., Xue, P., Sun, H. H. Y., Williams, I. D., Sharpless, K. B., Fokin, V. V., and Jia, G.,** 2005: Ruthenium-Catalyzed Cycloaddition of Alkynes and Organic Azides, *Journal of American Chemical Society,* **127**, 15998-15999.

[39] **Atkins. P. and Friedman R.,** 2005. Molecular Quantum Mechanics, Oxford University Press, Fourth Edition, pp 287-289, New York.

[40] **Hohenberg, P. and Kohn, W.,** 1964: Inhomogeneous Electron Gas**,** *Physical Reviews,* **136,** B864 - B871.

[41] **Hohenberg, P. and Kohn, W.,** 1965: Self-Consistent Equations Including Exchange and Correlation Effects, *Physical Reviews,***140**, A1133 - A1138.

[42] **Salahub, D. R. and Zerner, M. C.,** 1989. *The Challenge of d and f Electrons*, ACS, Washington, D.C.

[43] **Parr, R. G. and Yang, W.,** 1989. *Density-Functional Theory of Atoms and Molecules*, Oxford Univ. Press, Oxford.

[44] **Roothan, C. C. J.,** 1951: New Developments in Molecular Orbital Theory, *Reviews of Modern Physics*, **23**, 69 – 89.

[45] **Pople, J. A. and Nesbet, R. K.,** 1954: Self-Consistent Orbitals for Radicals, *Journal of Chemical Physics,* **22,** 571.

[46] **McWeeny, R. and Dierksen, G.,** 1968: Self-Consistent Perturbation Theory II, *Journal of Chemical Physics,* **49**, 4852-4856.

[47] **Becke, A.D.,** 1993: Density-functional thermochemistry III The Role of Exact Exchange., *Journal of Chemical Physics,* **98**, 5648-5652.

[48] **Jensen, F.,** 1999. Introduction to Computational Chemistry, John Wiley and Sons, pp 150-350, England.

[49] **Gonzalez, C. and Schlegel, H.B.,** 1989: An Improved Algorithm for Reaction Path Fallowing, *Journal of Chemical Physics,* **90,** 2154.

[50] **Gonzalez, C. and Schlegel, H.B.,** 1990: Reaction Path Following in mass-Weighted Internal Coordinates, *Journal of Physical Chemistry,* **94**, 5523.

[51] **Url-1** < *http://www.iupac.org/reports/1999/7110minkin/i.html*>, accessed at 10.01.2011.

[52] **Carpenter, J.E. and Weinhold F.,** 1988: Analysis of the Geometry of the Hydroxymethyl Radical by the "Different Hybrids for Different Spins" Natural Bond Orbital Procedure, *Theochem,* **169**, 41.

[53] **Carpenter, J.E.,** 1987, PhD thesis, University of Wisconsin, Madison, WI,.

[54] **Foster, J.P. and Weinhold, F.,** 1980: Natural Hybrid Orbitals, *Journal of American Chemical Society,* **102**, 7211-7218.

[55] **Reed, A.E. and Weinhold, F.,** 1983: Natural Hybrid Orbital Analysis Of Near Hartree-Fock Water Dimer , *Journal of Chemical Physics,* **78**, 4066-4073.

[56] **Reed, A. E. and Weinhold, F.,** 1983: Natural Localized Molecular-Orbitals, *Journal of Chemical Physics*, **83**, 1736-1740.

[57] **Reed, A. E., Weihstock, R. B. and Weinhold, F.,** 1985: Natural-Population Analysis, *Journal of Chemical Physics,* **83**, 735-746.

[58] **Carpenter, A. E. and Weinhold, F.,** 1988: The Structure of Small Molecules and Ions, *Plenum*, *227*-236.

[59] **Reed, A. E., Curtiss, L. A. and Weinhold, F.,** 1988: Intermolecular Interactions from a Natural Bond Orbital, Donor-Acceptor Viewpoint, *Journal of Chemical Reviews (Washington D.C.),* **88**, 899-926.

[60] **Lee, C. T., Yang, W. T., Parr, R. G.,** 1988: Development of the Colle-Salvetti correlation-energy formula into a functional of the electron density, *Physical Reviews B,* **37**, 785-789.

[61] Becke, A. D., 1993: Density-functional thermochemistry. III. The role of exact exchange, *Journal of Chemical Physics,* **98**, 5648-5652.

[62] **Miehlich, B., Savin, A., Stoll, H., and Preuss, H.,** 1989: Results obtained with the correlation energy density functionals of becke and Lee, Yang and Parr, *Chemical Physics Letters,* **157**, 200-206.

[63] **Frisch, M. J., Trucks, G. W., Schlegel, H. B., Scuseria, G. E., Robb, M. A., Cheeseman, J. R., Montgomery, J. A., Vreven, Jr., T., Kudin, K. N., Burant, J. C., Millam, J. M., Iyengar, S. S., Tomasi, J., Barone, V., Mennucci, B., Cossi, M., Scalmani, G., Rega, N., Petersson, G. A., Nakatsuji, H., Hada, M., Ehara, M., Toyota, K., Fukuda, R., Hasegawa, J., Ishida, M., Nakajima, T., Honda, Y., Kitao, O., Nakai, H., Klene, M., Li, X., Knox, J. E., Hratchian, H. P., Cross, J. B., Adamo, C., Jaramillo, Gomperts, R., Stratmann, R. E., Yazyev, O., Austin, A. J., Cammi, R., Pomelli, C., Ochterski, J. W., Ayala, P. Y, Morokuma, K., Voth, G. A., Salvador, P., Dannenberg, J. J., Zakrzewski, V. G., Dapprich, S., Daniels, A. D., Strain, M. C., Farkas, O., Malick, D. K., Rabuck, A. D., Raghavachari, K., Foresman, J. B., Ortiz, J. V., Cui, Baboul, A. G. , Clifford, S., Cioslowski, J., Stefanov, B. B., Liu, G., Liashenko, A., Piskorz, P., Komaromi, I.,RMartin, . L., Fox, D. J., Keith, T., Al-Laham, M. A., Peng, C. Y., Nanayakkara, A., Challacombe, M.,Gill, P. M. W., Johnson, B., Chen, W.,Wong, M.**

W., Gonzalez, C. and Pople J. A., 2004. Gaussian 03, Revision C.02, *Gaussian, Inc*., Wallingford CT.

[64] **Fukui, K.,** 1970: A Formulation of the Reaction Coordinate, *Journal of Physical Chemistry, **74**,* 4161.

[65] **Fukui, K.,** 1981: The Path of Chemical Reactions - The IRC Approach, *Acccounts of Chemical Research,* **14,** 363.

[66] **Foster, P., and Weinhold, F.,** 1980: Natural Hybrid Orbitals, *Journal of American Chemical Society,* **102,** 7211– 7218.

[67] **Reed, A., and Weinhold, E. F.,** 1983: Natural bond orbital analysis of near Hartree–Fock water dimer, *Journal of Chemical Physics,* **78**, 4066–4073.

[68] **Reed, A. E., Weihstock R. B., and Weinhold, F.,** 1985: Natural population analysis, *Journal of Chemical Physics,* **83**, 735–746.

[69] **Reed, A. E. andd Weinhold, F.,** 1985: Natural localized molecular orbitals, *Journal of Chemical Physics,* **83,** 1736– 1740.

[70] **Reed, A. E., Curtiss, L. A., and Weinhold, F.,** 1988: Intermolecular interactions from a natural bond orbital, donor-acceptor viewpoint, *Chemical Re*views, **88**, 899–926.

[71] **Majireck, M. M., and Weinreb, S. M.,** 2006: A Study of the Scope and Regioselectivity of the Ruthenium-Catalyzed [3+2]–Cycloaddition of Azides with Internal Alkynes, *Journal of Organic Chemistry*, **71**, 8680-8683.

[72] **Cenini, S., Gallo, E., Caselli, A., Ragaini, F., Fantauzzi, S., and Piangiolino,C.,** 2006: Coordination chemistry of organic azides and amination reactions catalyzed by transition metal complexes, *Coordination Chemistry Reviews,* **250**, 1234-1253.

CURRICULUM VITAE

Candidate's full name:	Esra BOZ
Place and date of birth:	26.09.1986 - İstanbul
Permanent Address:	Namık Kemal Mah. Köşk Sok. 9/3 Ümraniye- İstanbul
Universities and Colleges attended:	İstanbul Technical University, Faculty of Science and Letters, Chemistry.